ON THE STABILITY OF FLOW IN ROTATING PIPES

Hassan M. Nagib, et al

Illinois Institute of Te chnology
Chicago, Illinois

October 1969

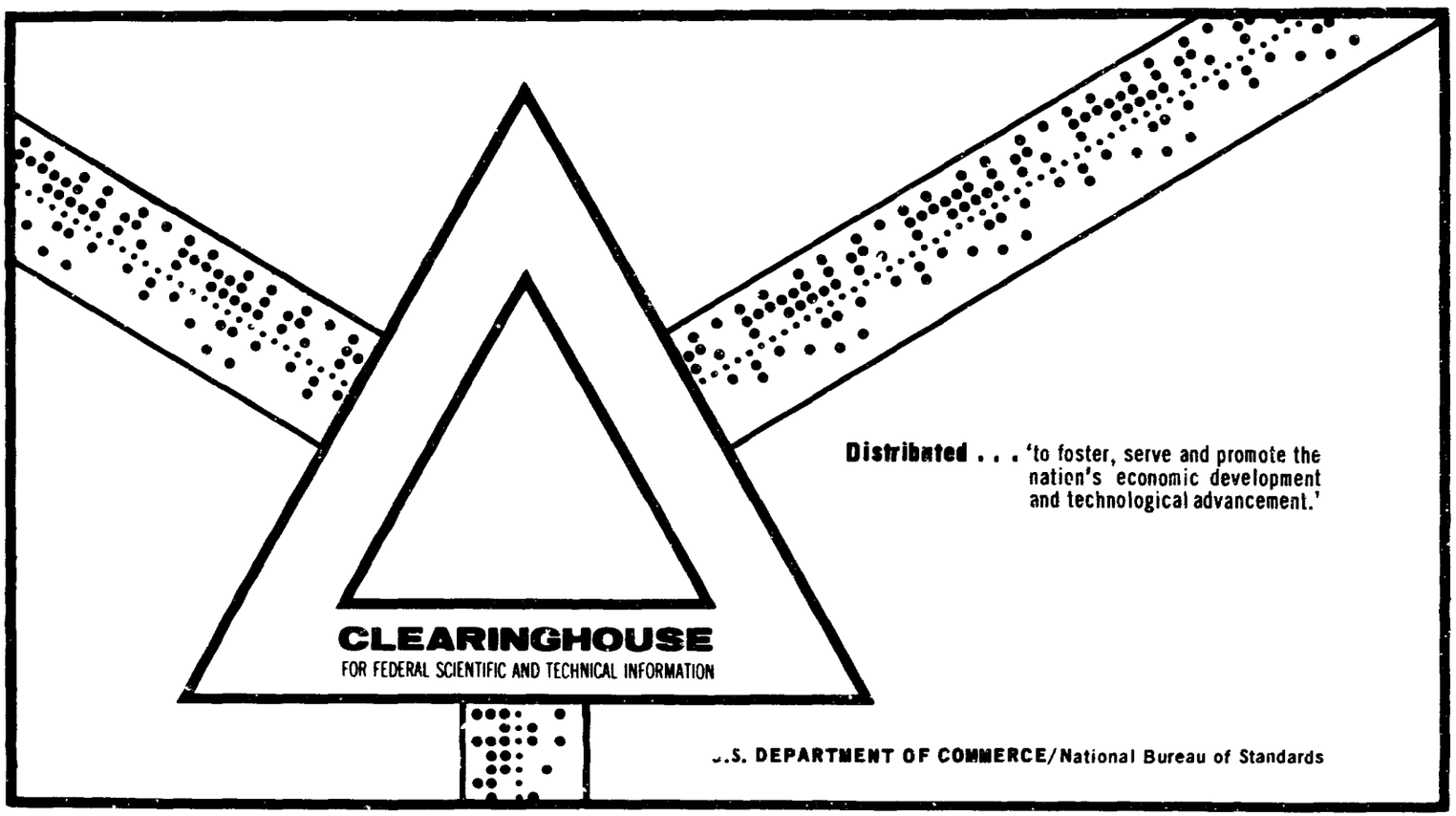

ARL 69-0176
OCTOBER 1969

Aerospace Research Laboratories

ON THE STABILITY OF FLOW IN ROTATING PIPES

H. M. NAGIB
L. WOLF, JR.
Z. LAVAN
A. A. FEJER

ILLINOIS INSTITUTE OF TECHNOLOGY
CHICAGO, ILLINOIS

Contract No. AF33(615)-67-C-1406
Project No. 7116

OFFICE OF AEROSPACE RESEARCH

United States Air Force

113

NOTICES

When Government drawings, specifications, or other data are used for any purpose other than in connection with a definitely related Government procurement operation, the United States Government thereby incurs no responsibility nor any obligation whatsoever; and the fact that the Government may have formulated, furnished, or in any way supplied the said drawings, specifications, or other data, is not to be regarded by implication or otherwise as in any manner licensing the holder or any other person or corporation, or conveying any rights or permission to manufacture, use, or sell any patented invention that may in any way be related thereto.

Agencies of the Department of Defense, qualified contractors and other government agencies may obtain copies from the

Defense Documentation Center
Cameron Station
Alexandria, Virginia 22314

This document has been released to the

- - - - - - - - - -

CLEARINGHOUSE
U.S. Department of Commerce
Springfield, Virginia 22151

for sale to the public.

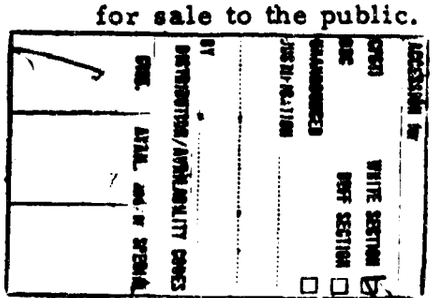

Copies of ARL Technical Documentary Reports should not be returned to Aerospace Research Laboratories unless return is required by security considerations, contractual obligations or notices on a specified document.

300 - December 1969 - CO455 - 104-2274

ARL 69-0176

ON THE STABILITY OF FLOW IN ROTATING PIPES

H. M. NAGIB
L. WOLF, JR.
Z. LAVAN
A. A. FEJER

ILLINOIS INSTITUTE OF TECHNOLOGY
CHICAGO, ILLINOIS

OCTOBER 1969

Contract No. AF33(615)-67-C-1406
Project No. 7116

AEROSPACE RESEARCH LABORATORIES
OFFICE OF AEROSPACE RESEARCH
UNITED STATES AIR FORCE
WRIGHT-PATTERSON AIR FORCE BASE, OHIO

FOREWORD

This is the final report on the experimental portion of the work performed under Contract No. F33615-67-C-1406, IIT Project No. 55019, "On the Stability of Flow in Rotating Pipes," covering the period of April 1, 1968 to April 1, 1969. The work was carried out for the Aerospace Research Laboratories, Office of Aerospace Research, United States Air Force, with Capt. J. A. Decaire as project monitor.

Contributors to this report are Mr. Hassan M. Nagib, Mr. Ludwig Wolf, Jr., Dr. Zalman Lavan and Dr. Andrew A. Fejer. Dr. Mark V. Morkovin provided valuable assistance throughout the course of this investigation.

ABSTRACT

The stability of flow in rotating pipes is investigated experimentally. The results of this investigation also have a bearing on the stability of flow in the core of swirling flows in stationary ducts and free vortices. Solid body rotation is found to have a destabilizing effect when superposed on a pipe entrance region axial velocity profile. The range of swirl ratios up to four is investigated using two different approaches: dye streaks visualization and hot-thermistor anemometry. As the swirl ratio is increased from zero to four, the axial Reynolds number at which laminar flow breaks down decreases from 2500 to 900. These results agree in trend with the limit axial Reynolds number value of 82.9 that was recently obtained by analytical investigations of the stability of a viscous fully developed axial velocity profile subject to a rapid, almost rigid rotation in pipes. The present results also suggest that the destabilizing trend due to solid body rotation may also hold for other axial velocity profiles and indicates a possible new mechanism of confined flow instability that takes place at lower Reynolds numbers than previously believed possible.

TABLE OF CONTENTS

Table of Contents (Cont'd)

LIST OF ILLUSTRATIONS

List of Illustrations (Cont'd)

LIST OF SYMBOLS

Symbol	Description
A	Cross section area
B	Constant defined on page 74
C	Constant defined on page 74
C'	Constant defined on page 74
D	Pipe inside diameter
E	Potential difference
E_o	Potential difference at zero flow velocity
G	Flow rate per unit area
g	Gravitational constant
K	Permeability
L	Length of pipe
ℓ	Length of porous plug
N_{Rz}	Axial Reynolds number defined on page 14
$N_{R\theta}$	Tangential Reynolds number defined on page 14
$N_{R\lambda}$	Reynolds number based on friction length defined on page 73
ΔP	Pressure difference
ΔP_r	Radial pressure gradient due to rotation
ΔP_z	Axial pressure drop
Q	Volumetric flow rate

List of Symbols (Cont'd)

R	Electrical resistance
R_o	Electrical resistance of cold thermistor
R_∞	Constant defined on page 80
r	Radial coordinate
T	Temperature
T_o	Constant defined on page 80
U, V, W	Velocity components in the r,θ and z direction
V_x, V_y, V_z	Velocity components in the x,y and z direction
x, y, z	Cartesian coordinates
z	Axial coordinate
α	Coefficient of shear resistance
β	Coefficient of inertial and compressible effects
Γ	Swirl ratio defined on page 14
γ	Angle, see Fig. 20
θ	Angular coordinate
λ	Friction length defined on page 73
μ	Absolute viscosity
ν	Kinematic viscosity
ρ	Density
Φ	Constant defined on page 73
ω	Angular velocity

CHAPTER I

INTRODUCTION

A. Literature Survey

Swirling flows in ducts are important flow phenomena from a practical as well as a fundamental point of view. These flows are of great relevance to rotating machinery, heat exchangers, energy and mass separation devices, nuclear rocket engines and other potential applications. It is of course essential in all such applications to predict under what conditions the flow will always be laminar and when it may or will undergo transition. The latter question is the problem of hydrodynamic stability, which in turn can be phrased as the stability to infinitesimal or finite disturbances. In some problems these two approaches yield results in close agreement while in others they differ widely. Since swirling flows are composed of axial and rotating motions, we first review the stability of these independent components and then consider the combined flow.

Axial or Pipe Flow

Reynolds[1] in his classical investigation, in 1883, concluded that the flow through circular pipes would be stable if a characteristic number associated with the flow is less than 2000.

(This characteristic number is referred to as Reynolds number.) Such a limiting minimum value for the flow to remain laminar under all conditions is commonly known as the critical Reynolds number. Several investigators attempted to obtain analytical solutions to this problem considering infinitesimal disturbances. No instability was found when axisymmetric as well as non-axisymmetric disturbances were considered with fully developed flow. Sexl,[2,3] Pekeris,[4] Sexl et. al.[5], Corcos et. al.[6], Lessen et. al.[7] and Gill[8] are a few of the investigators who studied this problem.

Corcos et. al.[6] investigated the stability of infinitesimal axisymmetric disturbances in fully developed flow in a pipe by treating the classic eigenvalue problem and concluded that all eigenvalues yield stable solutions and that for a given wave number and Reynolds number only a finite number of eigenvalues are present. These results appear to be substantiated by the experimental investigation of Leite,[9] who concludes that the flow is stable to small axisymmetric disturbances up to a Reynolds number of 13,000.

Lessen et. al.[7] investigated the stability of Poiseuille flow to non-axisymmetric disturbances (azimuthally periodic). Fox et. al.[10] investigated the same problem experimentally and found a minimum critical Reynolds number of approximately 2150.

Rotta[11] investigated the laminar and turbulent regimes as well as their structure in flow through pipes. He also studied the changes in the axial velocity profile associated with these flow regimes along the pipe.

Orr,[12] by means of applying the energy method to steady viscous motions of liquids in pipes, was able to find a limit Reynolds number value of 88 for sure stability of fully developed flow. Joseph et. al.[13] in their recent investigation found a yet lower value of 82.88 for such a limit using a more general approach.

Rotating Flow

Lord Rayleigh[14] presented his criteria for inertial instability of rotating fluids in 1916, where he considers purely rotating inviscid flow under axisymmetric disturbances. According to his criteria, an inviscid rotating flow is unstable if the sense of the local vorticity is opposite to the sense of the angular velocity. A different way of stating his criteria is: the stability of fluid motion in cylindrical strata requires only that the square of the circulation increases outwardly.

Taylor[15] extended this work to Couette flow and took into account the effect of viscosity. In his analysis, the small gap approximation was made and a criterion for

instability was obtained. Based on this analysis an instability in the form of torroidal vortices is to occur if a critical number known as the Taylor number is reached. It should be pointed out that this kind of instability cannot occur when the outer cylinder is rotating at a higher angular velocity than that of the inner cylinder. From this criterion it follows that the flow is to be stable if the inner cylinder is stationary or absent, and hence pure rigid body rotation is always stable to infinitesimal disturbances. Sparrow et. al.[16] extended this analysis to include wide gaps and rotation in opposite senses. For this phenomenon (Taylor instability) linear theory, finite disturbance theory and experiment are in excellent agreement. Coles[17] presented a thorough investigation of the same problem in relation to the different kinds of possible transition. He concludes that there exist two different kinds: Taylor's instability, and what appears to be regular turbulence. The latter occurs when the inner cylinder is stationary or rotating, and the outer one rotates at a very high angular velocity relative to the inner one. His work, in addition to its theoretical value, is an excellent reference to experimental investigations of rotating fluids. It should be pointed out that Taylor also observed the second kind of instability. It is believed that this instability is not due to eccentricities as it is stated in some of the

earlier works (Shultz-Grunow[18]), but is due to a different mechanism of instability than that of the Taylor instability. The eccentricities in such a mechanism represent time-dependent finite disturbances.

Swirling Flows

Chandrasekhar[19] developed a stability theory for swirling inviscid flows and attempted unsuccessfully to show that Rayleigh's criteria is also applicable to non-axisymmetric disturbances. Di Prima[30] extended this theory to viscous fluids between rotating cylinders with an axial flow and found that the critical Taylor number increases with increasing Reynolds number. Chandrasekhar,[21] Krueger et. al.[22] and Datta[23] studied the stability of swirling flows under small axisymmetric disturbances using the small gap approximation.

By extending Rayleigh's criterion Howard and Gupta[24] were the first to develop a stability criterion for non-dissipative swirling flows that has been extended to a large gap and non-axisymmetric disturbances. From this criterion it follows that solid body rotation as well as the fully developed Poiseuille flow in a pipe (considered separately) are stable under axisymmetric disturbances. Hughes and Reid[25] extended their analysis of axisymmetric disturbances in a narrow gap to include a wide range of Reynolds numbers.

Ludwieg[26,27] attempted to treat the stability of swirling inviscid flow confined to a narrow cylindrical annulus, considering non-axisymmetric disturbances. He shows that a small axial shear is sufficient to destabilize such a flow only if that flow is in solid body rotation. In his work Ludwieg[28] applied the criterion developed in the early studies to the case of flow over a delta wing.

Kiessling[29] extended Ludwieg's work to viscous fluids and found that the critical Reynolds number increases as the swirling flow deviates from solid body rotation.

Ludwieg,[30] using a complicated experimental apparatus, verified his stability theory and was able to observe a wave pattern of a helical shape. In his experiment the flow is confined between two concentric cylinders with a relatively small gap. The cylinders rotate in either direction and a continuous axial displacement is applied to the inner cylinder.

Pedley[31] extended the results of Howard et. al.[22] and showed that a cylindrically symmetric shear flow of an incompressible fluid subject to rapid, almost rigid rotation about its axis is unstable to infinitesimal inviscid non-axisymmetric disturbances. He succeeded in obtaining this result using non-axisymmetric linear disturbances (the axisymmetric analysis failed to show this). It should be recalled that Ludwieg[25,26] obtained the same result using the narrow gap

approximation. In Pedley's[31] analysis the flow is bounded externally by a rigid cylinder and internally it may be bounded by another rigid cylinder or the axis of the outer cylinder. In his later work Pedley[32] investigated the same flow considering a viscous fluid and showed that the flow is unstable for Reynolds numbers greater than approximately 82.9. Strohl[33] investigated the same problem as in Pedley's[32] work using a more general numerical approach and obtained the same results.

There is a real surprise in Pedley's[32] and Strohl's[33] work in that they contradict the widespread belief that rotation always has a stabilizing effect. A conclusion of their work is that a slow Poiseuille flow in a pipe has a destabilizing effect on a rapid, rigid body rotation and that a rapid, rigid body rotation has a destabilizing effect on a slow Poiseuille flow. It should be noted from the results of earlier works that each of these flows is stable by itself.

The stability of axial flow in rotating pipes was investigated experimentally by White[34] and Cannon et. al.[35] The two investigations conclude that rotation is stabilizing. It is believed that their results disagree with the analysis of Pedley[32] and Strohl[33] because solid body rotation was not obtained in their experiments, and regions of recirculation were present. It was therefore proposed to construct an experiment that will be free of these objections and will more closely approximate the study of stability of an axial flow with a superposed solid body rotation.

B. Definition of the Problem

An attempt is made toward the experimental investigation of the hydrodynamic stability of flow in rotating pipes. The flow is to be a solid body rotation superposed on an axial velocity profile that is free of recirculation. A fully developed profile would have been desirable; however this requires a cumbersome length or an intricate entrance configuration. It was therefore decided to use an axial velocity profile characteristic of pipe entrance regions. The working fluid is water and a range of axial Reynolds numbers up to 7000 is to be investigated. The classification of the flow condition into laminar and turbulent regimes is carried out by dye streak visualization and hot-thermister probes. When the regular laminar flow pattern breaks down slightly the flow is said to be in the transition regime, and when a continuous state of irregular motions is reached the flow is referred to as turbulent. It should be pointed out that these definitions are not precise. A more precise and detailed study of the structure of the disturbed flow is one of the problems contemplated for future investigation.

CHAPTER II

EXPERIMENTAL APPARATUS

The rotating pipe apparatus shown in Fig. 1 was designed with the following objectives in mind.

1) To control conditions at the inlet and outlet of the rotating pipe in order to obtain a flow of solid body rotation and an axial flow which is free of reverse axial components.

2) To provide a pipe of sufficiently large diameter in which quantitative measurements of the flow field could be obtained and which facilitates visual diagnostic approaches.

3) To allow a wide range of operating conditions.

4) To permit the possibility of using different fluids as working media.

The apparatus and the associated equipment are described below.

A. Rotating Pipe

The rotating pipe apparatus consists of a 73-3/4 inch long lucite pipe. The pipe has a 3-1/4 inch inside diameter and 3-3/4 inch outside diameter (L/D $\simeq$ 23). The tolerance, as stated by the manufacturers, is $\pm$ 0.020 inches. However, the

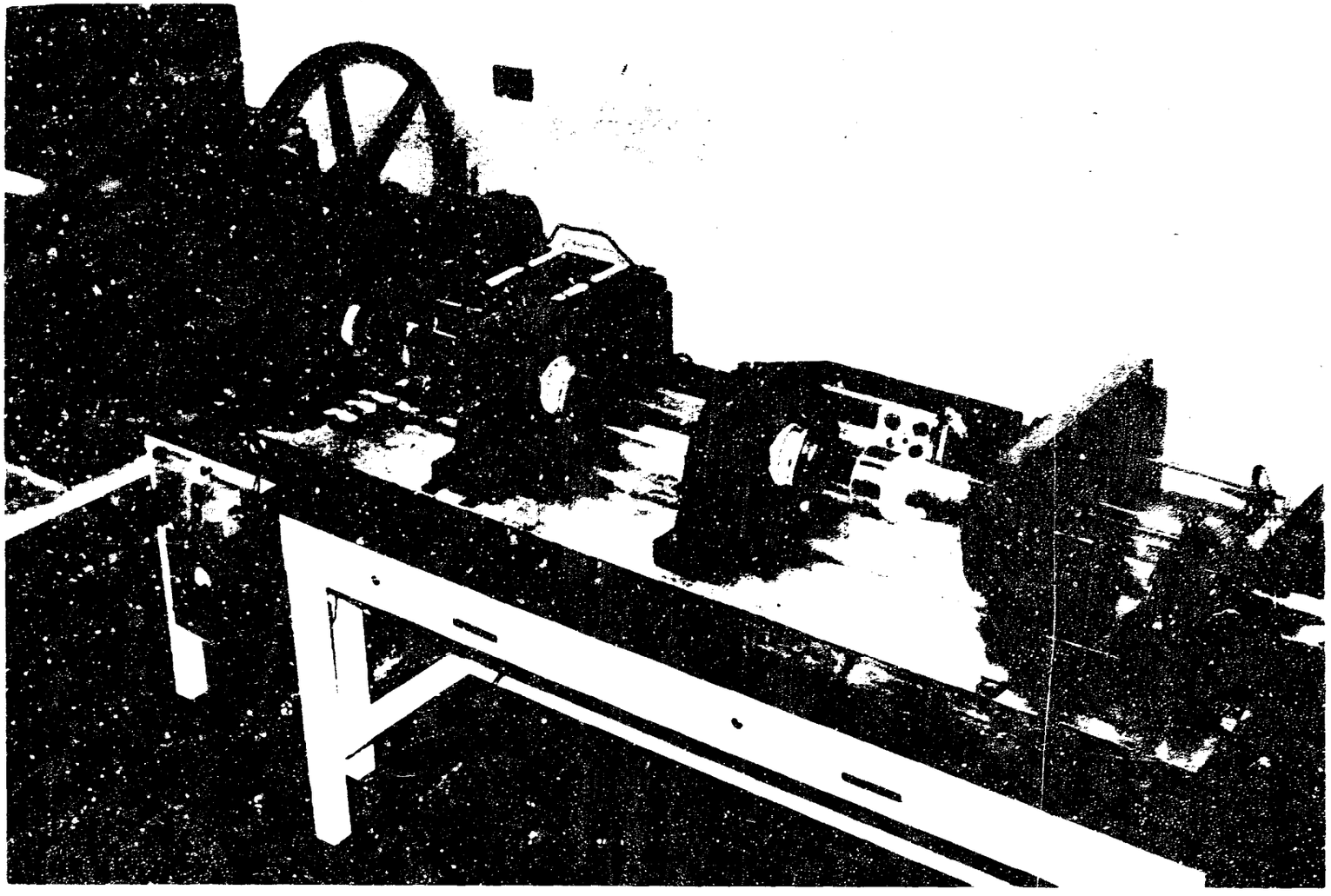

FIG. 1. ROTATING PIPE APPARATUS

main tolerance is in the wall thickness, while the inside diameter is accurate to within $\pm$ 0.005.

For any experimental investigation connected with the study of the stability of rotating flows, it is found (see Coles[18]) that the tolerance in the concentricity between the axis of the rotating body and the axis of rotation should be minimal. The pipe is therefore constructed so that it will rotate about an axis that best coincides with the center of the inside diameter along the length of the pipe. This is achieved by cementing stainless steel sleeves to the outside diameter of the pipe. The sleeves are machined to an outside diameter of $4\ ^{+\ 0.0000}_{-\ 0.0015}$ inches and a maximum tolerance on their concentricity with the center of the inside diameter of $\pm$ 0.005 inches. This procedure is found to be time-consuming and relatively expensive.

The sleeves are used to support the pipe inside five self-aligning ball bearings. Two of the five bearings are located close to each other on one long sleeve, which is also used to mount the drive mechanism pulley (located between the two bearings). These two bearings are located as close to each other as the thickness of the pulley permits, and the remaining bearings are equally spaced. The five bearings are four inch diameter self-aligning ball bearings. Four of them are medium-duty pillow blocks and the fifth is a medium-duty

flange unit. The flange unit bearing is mounted on a 1-1/2 x 13 x 17 inch aluminum plate. Rotating oil seals are mounted at each end of the pipe.

A pressure-tight settling chamber is provided at the inlet of the pipe, while an open tank is used at the outlet. The pressure-tight chamber is made of an 11 inch long 7-1/4 inch inside diameter and 8-1/4 inch outside diameter lucite tube. The chamber is bounded on the downstream side by the aluminum plate on which the flange unit bearing is mounted and a 1 x 10 x 10 inch aluminum plate from the upstream side.

The flow supply line is connected to the upstream face of the pressure-tight chamber and a flow control valve is located a small distance upstream of the aluminum plate in the supply line. The downstream open tank is made of 1-1/2 inch plexiglass. The dimensions of the open tank are 15 x 20 x 36 inches. The entire assembly is mounted on a 20 inch wide, 12 feet long, aluminum channel resting on three lab tables. The drain, supply and connecting flow lines consist of one-inch diameter tygon tubing. The downstream open tank is equipped with a drain system that can maintain a constant head in the tank for all axial Reynolds numbers used. The system is a two-level drain with a valve controlling the lower drain, which is at a level higher than that required to keep the rotating pipe filled at all times.

The apparatus is equipped with a high head settling tank that can be used for temperature control, as well as treating the water to eliminate the color from the dye injected when operating in a recirculating mode. The settling tank can also be used to eliminate some of the air bubbles in the water.

When assembling the rotating pipe apparatus, the bearings were aligned and the pipe was leveled horizontally within a tolerance of $\pm$ 0.005 inches, by means of shimming the bearings. In aligning the bearings, piano wire, under tension, was used. It is felt that this procedure, although introducing some stresses in the lucite pipe, is necessary to insure that the pipe rotates concentrically about its axis.

The rotating pipe is equipped with porous plugs at both inlet and outlet in an effort to create a flow field of solid body rotation. It can be argued that if the pressure drop across the porous plug, due to the axial flow, is large in comparison to the radial pressure gradient associated with the pipe rotation, the flow downstream of the plug should be free of reverse axial components. In addition, if the plug is of uniform thickness, the flow field downstream of it, (up to some swirl ratio) should approximate plug flow superposed on solid body rotation. This limiting swirl ratio is governed primarily by the porosity of the plug as well as the other properties.

The porous plugs used are made of General Electric low-density nickel foametal. This material was chosen after different types of porous materials were investigated analytically and experimentally. The upstream plug is taken from a one-inch thick slab and the downstream plug from a two-inch thick slab. The plugs are 3-1/4 inch in diameter and are made to rotate with the pipe by placing them inside the ends of the pipe and cementing them with RTV. The pore size of the porous material is in the range between 0.020 inch and 0.100 inch. There are from 11 to 25 pores per lineal inch. The porous material is manufactured by means of foaming the nickel and is shaped by molding. The material has a bulk density of 2% of the solid nickel density. The foametal is also available in other metals, such as copper, and in a wide range of density, ranging from 2% to 65%. Although all the technical properties are supplied by the manufacturers, they are not available for the low density range (below 20% density). The material can be easily cut with a band-saw or other wood-working tools. The manufacturer recommends impregnating the material in paraffin before machining and removing the paraffin after machining is finished by soaking the material in degreasing solution. This procedure was not used and direct machining on the lathe was carried out successfully.

The pressure drop across the porous plugs was measured as a function of the flow velocity. The measurements show that it is proportional to the square of the flow velocity and is independent of the speed of rotation in the range of the present experiments. A simplified analytical approach is used to extend these results to the following more general and useful relation (see Appendix A).

$$\frac{\Delta P_r}{\Delta P_z} \doteq 0.004 \quad \Gamma^2 \qquad \text{II.1}$$

where Γ is the swirl ratio and is defined by the ratio of the tangential Reynolds number to the axial Reynolds number.

The tangential Reynolds number $N_{R\theta}$ is defined by

$$N_{R\theta} = \frac{VD}{\nu} = \frac{\omega D^2}{2\nu} \qquad \text{II.2}$$

where V is the maximum tangential velocity and the axial Reynolds number N_{Rz} is defined by

$$N_{Rz} = \frac{\bar{W}D}{\nu} \qquad \text{II.3}$$

where $\bar{W}$ is the mass flow average of axial velocity, ΔP_r is the radial pressure difference due to the pipe rotation, and ΔP_z is the pressure drop due to axial flow across one-inch of the porous material used. The ratio of the pressure gradient associated with the pipe rotation, to the pressure drop across the porous plug, due to the axial flow, remains much smaller than unity (e.g., 1/100), if the swirl ratio does not exceed a value of approximately four (based on a one-inch thick porous plug). Since the upstream plug is one-inch thick, one would expect the plugs to be effective in imparting the solid body rotation only up to swirl ratios of approximately four.

B. Drive Mechanism

In order to allow rotation of the pipe over the range of tangential Reynolds numbers under investigation in a stable and accurate manner, a complicated drive mechanism has been devised.

The reason for this can be explained as follows. For a pipe with an inside diameter of 3-1/4 inches, using water as the working fluid, a rotational speed of about 0.27 RPM's corresponds to a tangential Reynolds number ($N_{R\theta}$) of 100. A commercially available 1-1/2 horsepower variable-speed D.C. shunt motor, was found to operate at satisfactory stable speeds, over an RPM range of approximately 30 to 1400 RPM's. This

requires a speed reduction ratio of approximately 300 to 1, in order to provide operation at the required range of tangential Reynolds numbers.

The drive mechanism used provides a range of speed reduction ratios as high as 400 to 1 and as low as 13 to 1. This offers stable operation at tangential Reynolds numbers ranging approximately from 25 up to 40,000. The fluctuation in the rotational speeds using this drive mechanism is found to be approximately 2%.

The D.C. shunt motor electrical supply and speed control unit consists of the components shown schematically in Fig. 2. The speed control of the motor is carried out by using the armature-terminal-voltage control system. (This is the same control system used in the Ward Leonard system.) This control method, offering both constant torque and constant horsepower speed control, utilizes field control and armature-voltage control. The control panel for the D.C. shunt motor is shown in Fig. 3a.

The motor drives, through two pulleys and a V-belt, a variable reduction speed hydraulic transmission (Vickers 3/4 H.P. Model No. TR8-HR18-F18-20 Hydraulic transmission unit). This variable reduction speed hydraulic transmission offers reduction ratios from 1 to 1 and up to 30 to 1 (see Fig. 3c).

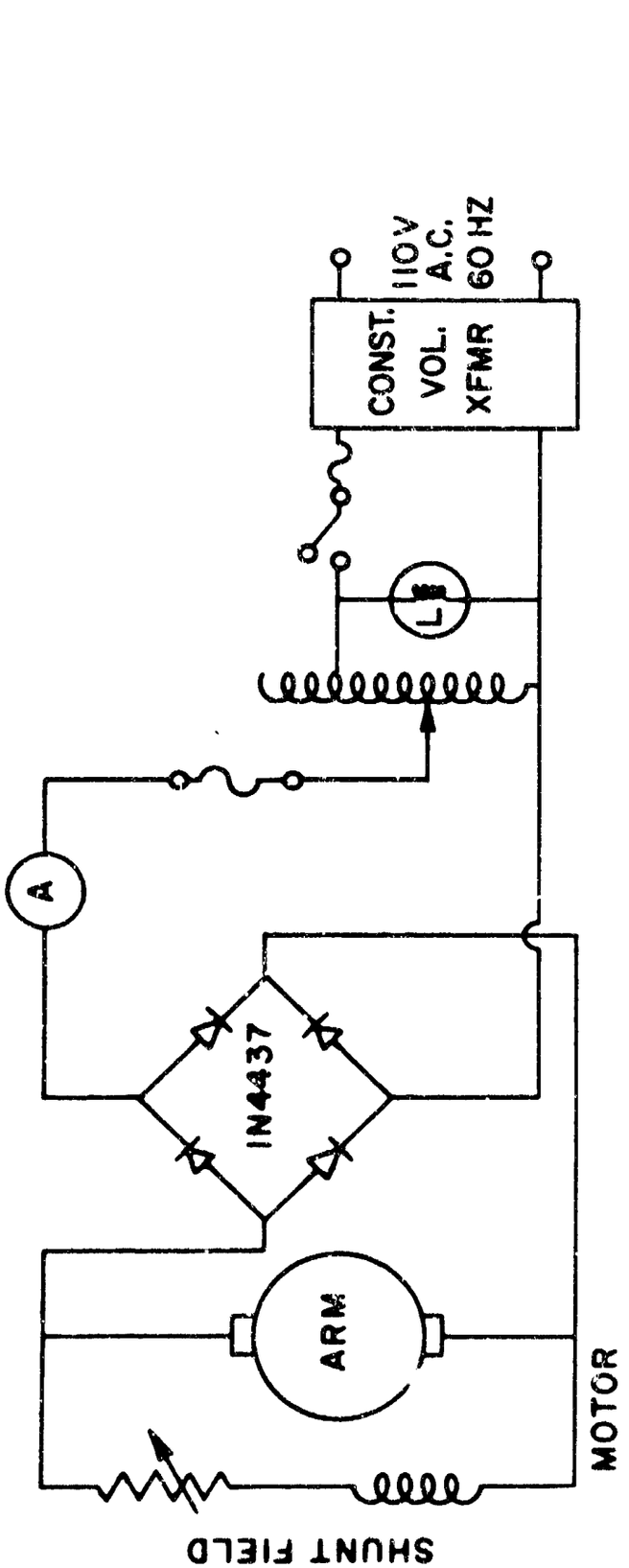

FIG. 2. ELECTRICAL SUPPLY AND SPEED CONTROL UNIT FOR D.C. MOTOR.

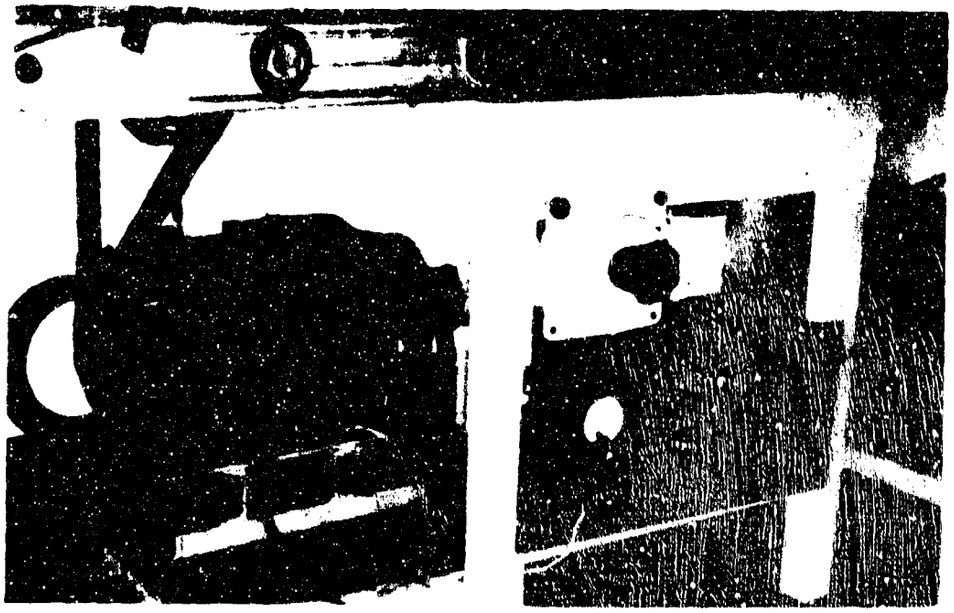

A. D.C. MOTOR AND CONTROL PANEL

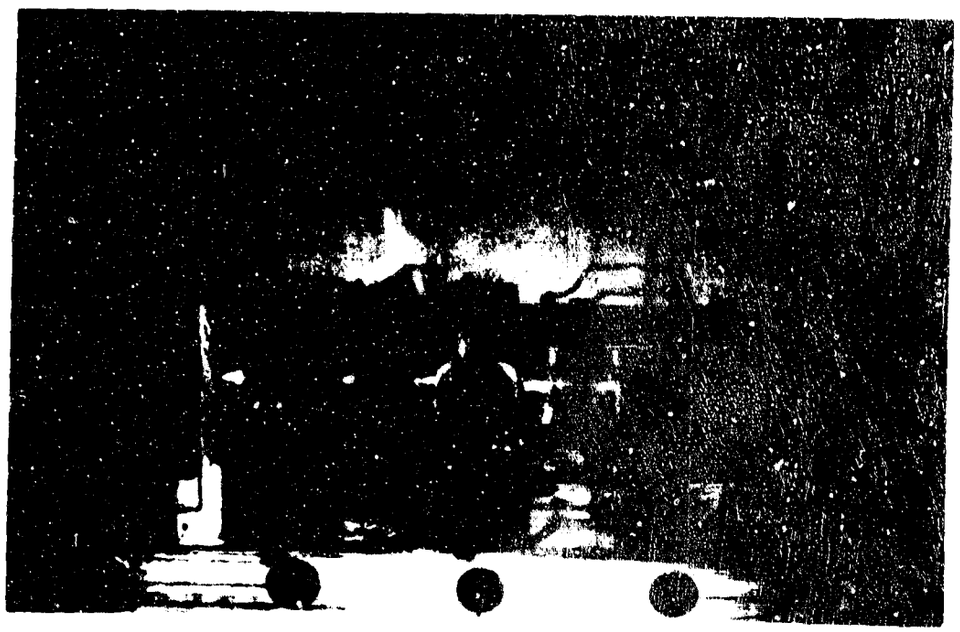

B. DRIVE MECHANISM GEAR BELT AND PULLEY MOUNTED ON ROTATING PIPE

FIG. 3. DRIVE MECHANISM COMPONENTS

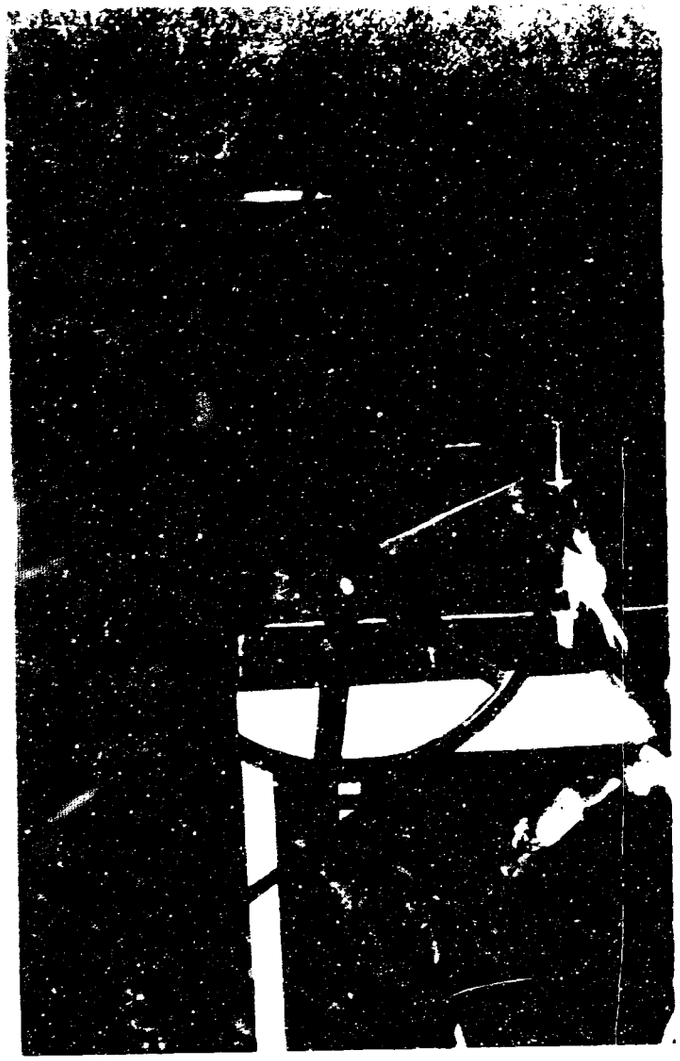

C. COMPONENTS OF DRIVE MECHANISM

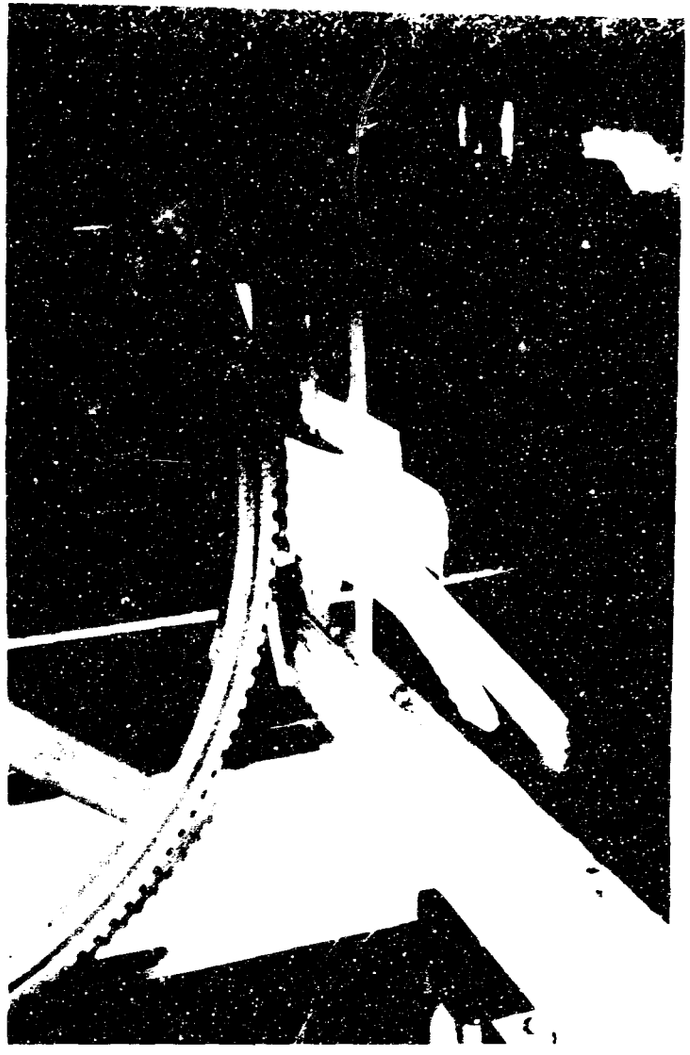

D. MICRO SWITCH MOUNTED AGAINST LARGE GEAR PULLEY

FIG. 3. (CONT'D) DRIVE MECHANISM COMPONENTS

The variable reduction speed hydraulic transmission drives the rotating pipe through a transmission consisting of four gear belt pulleys and two gear belts (timing belts). The four gear belt pulleys have pitch diameters of 2.865 inches, 24.828 inches, 5.013 inches, and 8.913 inches, respectively. The gear belts and pulleys provide a speed reduction ratio of approximately 13 to 1. The two intermediate pulleys located between the pulley on the output shaft of the hydraulic transmission and the pulley mounted on the rotating pipe, are mounted on a common one-inch diameter steel shaft. The shaft rotates inside two one-inch block bearings attached to aluminum channels on which the whole apparatus is mounted. All the components of the drive mechanism are shown in Fig. 3.

The rotational speed measurements are monitored by means of a microswitch indicating the rotational speed which is actuated by the largest gear pulley (see Fig. 3d). A D.C. voltage source (a 22-1/2 volt battery) and an electronic counter (Hewlett-Packard 5233L digital counter) are used in connection with the microswitch. The schematic diagram in Fig. 4 shows the electric circuit used in the rotational speed measuring instrumentation. The counter output is in kilocycles, that can be converted to either RPM's or tangential Reynolds numbers. For high rotational speeds the microswitch arrangement is replaced with a magnetic pickup, placed against

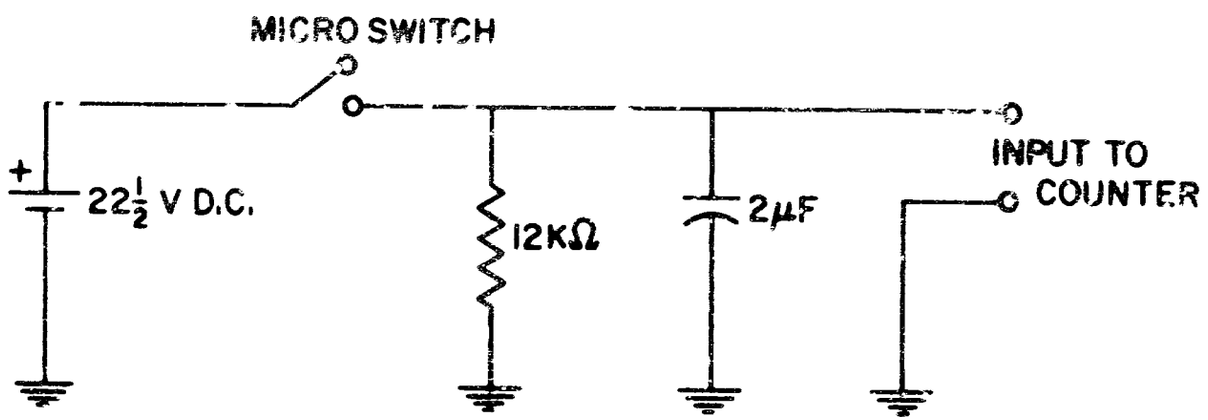

FIG. 4. ELECTRIC CIRCUIT FOR MEASURING THE PIPE ROTATIONAL SPEED.

the same gear pulley. Within the operating range, both the microswitch and the magnetic pickup circuitry offer an accuracy in the rotational speed measurements of approximately 0.1%.

The drive mechanism described above offers numerous control possibilities. By proper adjustments one can achieve the required tangential Reynolds number at operating conditions that are almost free of vibrations. Observation of the free surface in the downstream open tank, even the presence of slight vibrations in the assembly, can be readily detected with the naked eye. Adjustments must then be made to eliminate these vibrations since the absence of noticeable vibration is essential in an investigation concerned with stability.

C. Modes of Operation

The apparatus can be operated in a single pass mode where water from the building supply line passes through the apparatus to a drain. It can also be operated in a recirculating mode with the water being recirculated through the apparatus by a centrifugal pump. The pump is capable of delivering a head of 30 feet of water at a rate of about nine GPM's. This arrangement permits the adaptation of the apparatus to a range of different operating conditions and to different working fluids.

The single pass mode offers a higher range of axial Reynolds numbers, since the supply line pressure is higher than the head

delivered by the centrifugal pump. With water as the working fluid, the single pass mode can be operated at axial Reynolds numbers ranging from 0 to 12,000 and the recirculating mode can be operated at axial Reynolds numbers rarging from 0 to 7,000.

When dye injection visualization is used the single pass mode is preferable since recirculation in this case is practically impossible over a long period of time. In that case the dye injected would, within a short time, color the water in the system and the visibility of dye streaks would rapidly diminish with time.

There are however, several problems associated with the single pass mode:

1) The difference between the supply line water pressure and the room pressure. Due to this difference in pressure, a large number of air bubbles are formed in the pipe, which leads to problems with both the dye visualization and the hot-thermistor anemometry. In the case of the dye, the bubbles tend to disturb the dye streaks; and, in the case of the thermistor, the bubbles cause a large amount of noise in the output signal.

2) The fluctuation in the supply line pressure. This is especially apparent during the day, and it hinders the accurate adjustment of the flow rate.

The recirculating mode provides a very stable and quiet operation. Unless dye is injected or the thermistor output is observed, a person standing next to the apparatus cannot detect the flow, except by observing the flowmeters.

Using the recirculating mode, the flow rate can be controlled to within 0.5% in the operating range of the present investigation. The air bubble problem is also eliminated here.

The only problem connected with the recirculating mode is the energy supplied to the system by the pump, which tends to slowly raise the temperature of the water. Although this problem did not have great effect on the stability readings taken by the thermistor, it had some effect on the measurement of axial and tangential velocity fields. (This is discussed in more detail in Appendix B.) To minimize this problem, the system is left running for a long time, (until the water temperature reaches its equilibrium level) before performing any experiments.

For the above mentioned reasons, and in view of the fact that the present investigation is concerned with stability, the recirculating mode has been chosen for the quantitative measurements using the thermistor probes.

The flow rate through the apparatus is monitored by a rotameter at low flow rates and by a turbine-type flowmeter

(Potter Aero. Corp. Model 5/8-5570) at high flow rates. The range of measurements of both meters overlap in the range of axial Reynolds numbers from 1,300 up to 4,200. The two flowmeters combined can measure axial Reynolds numbers ranging from 80 to 14,500. Both meters are calibrated in the apparatus and offer the accuracy in the axial Reynolds numbers measurements stated above. The output of the turbine-type flowmeter is monitored by means of a Hewlett-Packard 5233L digital counter. The output is linear and is in kilocycles, which can be converted to axial Reynolds numbers. The flowmeters and the digital counter are shown in Fig. 5a.

D. Dye Injection

The rotating pipe inlet is equipped with dye injection probes. The probes are made of 0.026 inch inside diameter and 0.042 inch outside diameter stainless steel tubing. The dye probes are located at four radial positions. The innermost one is on the axis of the rotating pipe, and the outermost is in the vicinity of the wall (approximately 1/16 inch from the wall). The two other probes are located at equal distances between these two (see Fig. 5b).

The probes are joined at their upstream ends and connected to the dye supply tube. The connecting and supply tubes are made of 1/16 inch inside diameter and 1/8 inch outside diameter

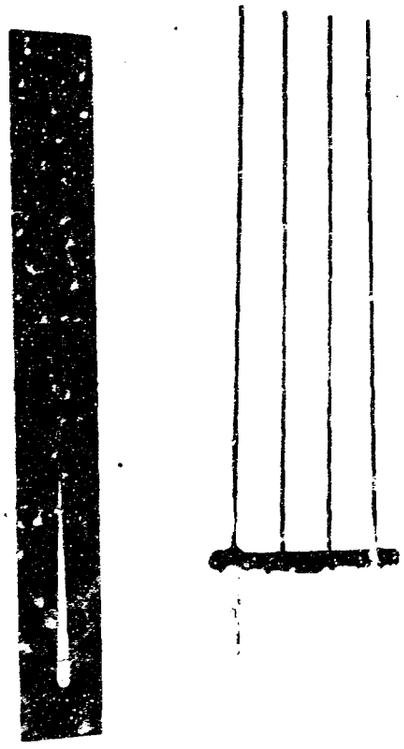

A. FLOWMETERS AND DIGITAL COUNTER

B. DYE INJECTION PROBES

FIG. 5. FLOWMETERS AND DYE INJECTION PROBES

stainless steel tubes. All the joints are made by means of silver soldering. The probes pass through the porous plug inside four stainless steel tubes of 1/8 inch inside diameter, attached to the porous plug by means of epoxy. These tubes serve as bearings for the probes. In mounting these tubes, extra care was taken to have all four tubes parallel to the axis of the plug and hence to each other. The probes were then placed inside the sleeves through the porous plug and tested outside the apparatus. By injecting water through the probes and observing the emerging jets, it was found that within the length of the rotating pipe (6 feet) the jets remained parallel and at equal distances from each other. A picture of the dye injection probes mounted inside the sleeves and through the upstream porous plug can be seen in Fig. 6a.

A short length of a larger diameter stainless steel tube (1/4 inch outside diameter) is silver soldered to the supply tube. (The 1/4 inch outside diameter tube permits the use of the smallest commercially available oil seal.) The oil seal is used to serve both the functions of the bearing and seal. The seal is press-fitted at the end of the dye pressure chamber.

The dye pressure chamber is cylindrical and is made of aluminum. It is mounted on the upstream plate of the pressure-tight settling chamber, located at the inlet of the rotating pipe. The dye is supplied to the dye pressure chamber by means of

A. DYE PROBES MOUNTED THROUGH INLET POROUS PLUG

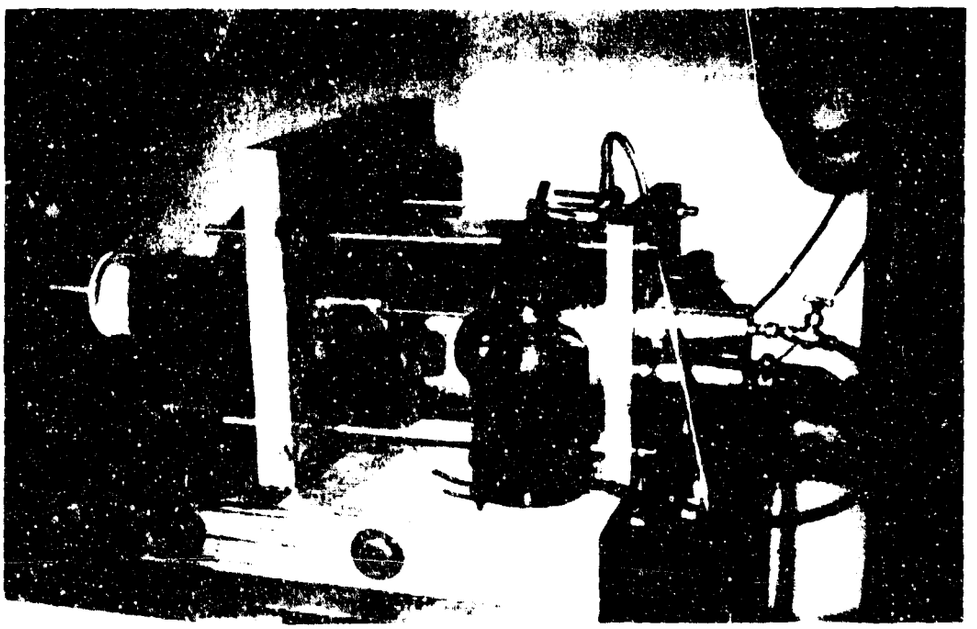

B. INLET CHAMBER WITH DYE INJECTION COMPONENTS

FIG. 6. DYE INJECTION COMPONENTS

tygon tubing from a large glass container and the amount flowing is controlled by a precision needle valve. Pressure is applied to the container using a rubber hand pump. The dye injection apparatus is shown in Fig. 6b.

The dye is injected a small distance downstream of the downstream face of the porous plug. Since the plug rotates with the tube, it appears that the dye is injected with no tangential velocity relative to the flow.

The dye used in these studies consists of malachite green crystals disolved in water. The density of the dye should be the same as that of water. Alcohol is added to the dye solution to effect density corrections. This is, however, an infrequent occurrence since the amount of crystals needed to give the dye its color is very small. The dye has a bluish-green color and does not lose its color even if left for several days.

The two main problems encountered in using the dye can be summarized as follows: first, a high relative axial velocity between the dye jet and the flow velocity may lead to dye jet instability. This instability was found to be a function of the relative velocity only, which in turn is a function of the difference between the dye injection pressure and the pressure of the flow at the location of the injection. It is also found that this instability may occur in laminar or turbulent conditions in the flow field. By careful observation

(see Fig. 7), one can differentiate between the turbulence in the flow field and the dye instability, since the latter has smaller scale eddies. This problem is eliminated by carefully controlling the pressure applied to the dye so that the axial velocity of the dye is the same as the axial velocity of the flow.

The second problem, which is less serious, is the differential in size and resistance between the dye probes. This can also be seen from Fig. 7, where the dye jet instability is occurring in some of the dye streaks and not in the others.

E. Instrumentation

In a recent investigation of the stability of Hagen-Poiseuille flow to non-axisymmetric disturbances by Fox et. al.,[10] hot-thermistor anemometry was used. The probes were used in a constant current mode to achieve a high sensitivity in measuring the velocity fluctuation. The working fluid used in this investigation is water. In comparison to this study, Leite[9] investigated the stability of the same flow to axisymmetric disturbances using air as the working fluid. In his investigation, Leite used hot-wire anemometry. Both investigations yield positive and successful results.

These investigations influenced strongly the choice of the instrumentation used in the present investigation. Although Fox et. al.[10] concluded that they are continuing their experiment

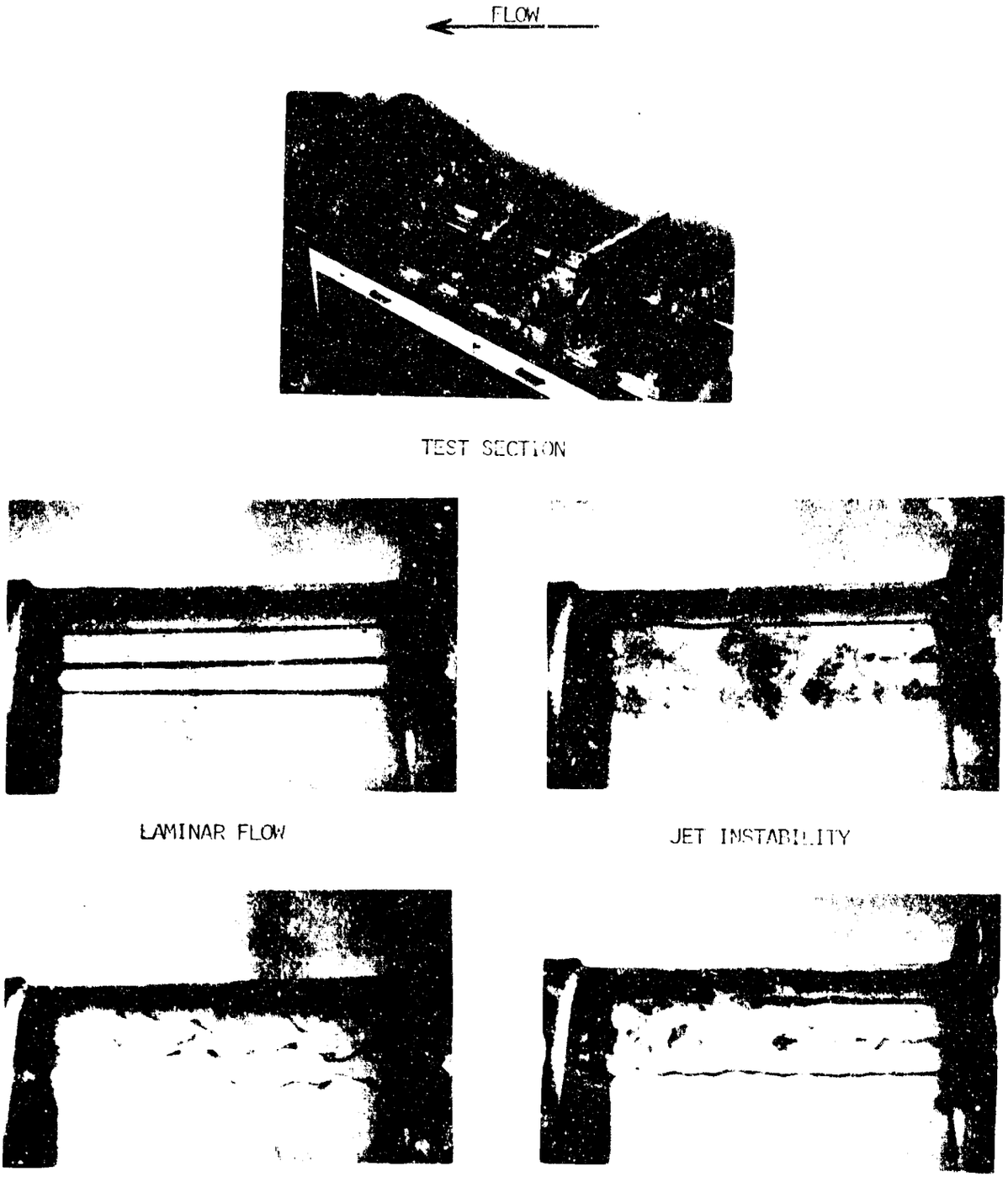

FIG. 7. DYE STREAK INSTABILITY AT LAMINAR AND TURBULENT AXIAL REYNOLDS NUMBERS WITH NO ROTATION

using wedge-shaped film probes with the hope of better results, adequate results were obtained using the hot-thermistor anemometry as reported in their investigation. In view of this, it was decided to use hot-thermisotr anemometry for the present investigation. This decision was supported by the results of a survey of literature on hot-thermistor anemometry. The main conclusions of this survey and other information on hot-thermistor anemometry are discussed in Appendix B.

In short, thermistors were chosen for this investigation since their high electrical resistance permits easy filtering of noise introduced by brushes and slip rings and makes possible the use of inexpensive and convenient electronics. They also offer, in water, the possibility of spatial resolution and noise levels that are better by an order of magnitude than those obtainable with platinum film probes. The probes are rugged, inexpensive and are commercially available. The major problem encountered is their low frequency responses. This however, does not limit their usefulness in determining transition from laminar to turbulent flow regimes. The probes were used in a constant current mode.

The different types of thermistor probes used are shown in Fig. 8. All the probes were commercially acquired, but additional work was performed on them to make them suitable for the mounting used in the rotating pipe apparatus.

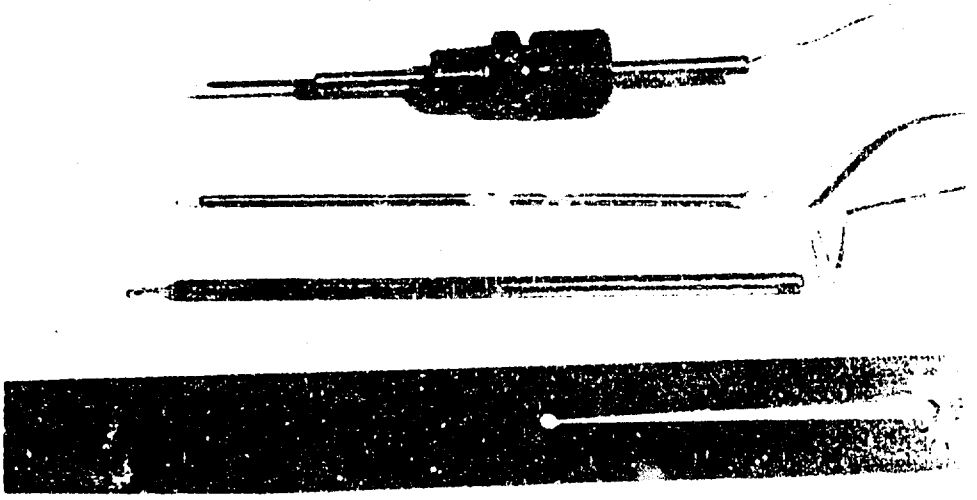

A. PROBE 4, 1 AND 2 (FROM TOP TO BOTTOM)

B. PROBE 4 MOUNTED INSIDE TEFLON SEAL

FIG. 8. THERMISTOR PROBES

The slip rings and brushes are homemade, though the underlying idea is related to mercury-wetted slip rings that are commercially available. The slip rings are made of two 1/2 inch thin sheets of brass. Each sheet is cemented to the outside of the pipe (around its circumference) and is joined by soldering. The brushes are two 1/2 inch ribbons made of brass screening. The ribbons are wrapped around the slip rings and connected to the two electric terminals located on a fixed rod mounted next to the rotating pipe (see Fig. 9a).

The brushes are sprayed with water which remains in the form of droplets (due to surface tension between the tiny square openings of the screen material). The amount of noise produced by the brushes is very low and can be suppressed very easily using an R-C filter, since it is of a much higher frequency than the output of the thermistor probe. A single application of water to the brushes is adequate for three hours of continuous operation.

The output of the thermistor anemometers is connected to the following instruments (shown in Fig. 9b):

1) Hewlett-Packard 3440A digital voltmeter equipped with a 344A D.C. multi-function unit to measure the D.C. component of the output.

2) DISA type 55D35 RMS unit to measure the root-mean-square of the A.C. component of the output.

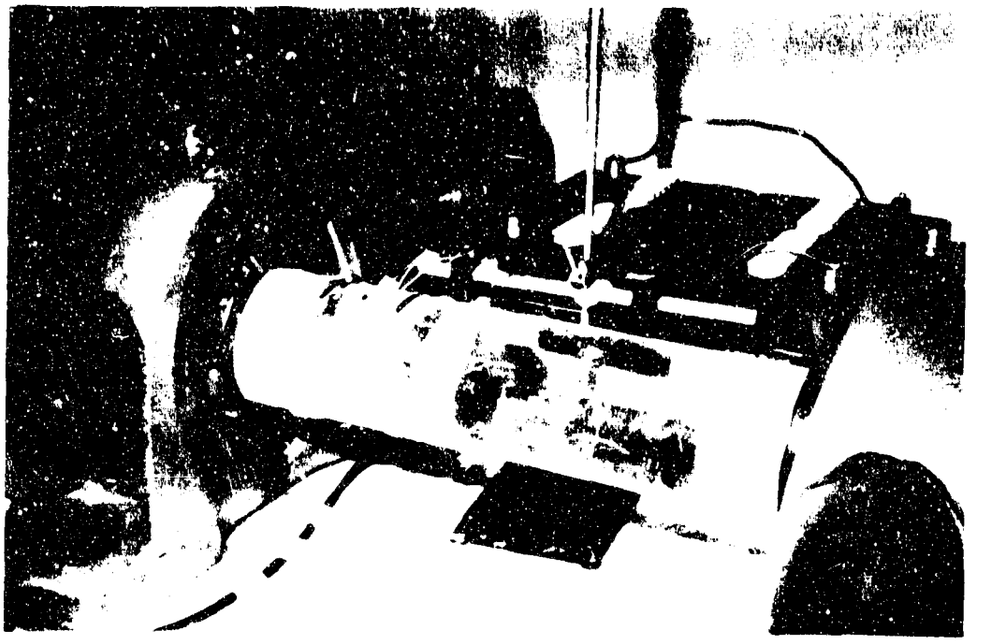

A. SLIP RINGS AND BRUSHES

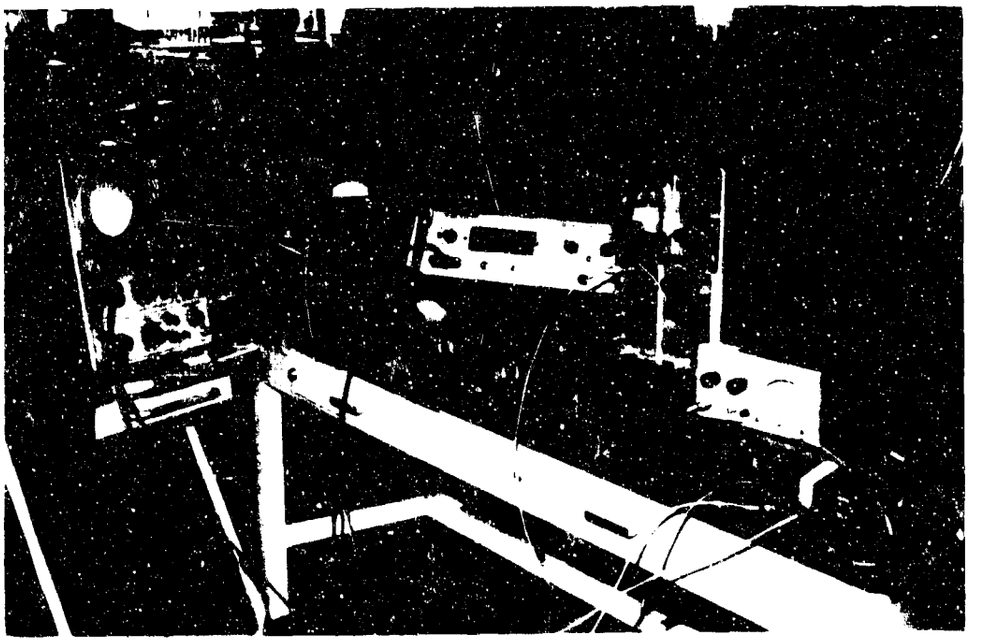

B. ANEMOMETRY MONITORING INSTRUMENTS

FIG. 9. ELECTRICAL INSTRUMENTATION COMPONENTS

3) Tektronix type 502A dual-beam oscilloscope to monitor the output.

4) Tektronix type 564 storage oscilloscope equipped with type 3A3 dual trace differential amplifier unit and a type 2B67 time base unit to store the output for taking pictures such as are shown in Fig. 16.

5) General Radio type 1564-A Sound and Vibration analyzer to analyze the frequency of the output.

CHAPTER III

EXPERIMENTAL RESULTS

In the present investigation the study of the stability of flow in rotating pipes is approached by means of two techniques: diagnostic dye streak flow visualization and quantitative hot-thermistor anemometry. The diagnostic flow visualizations are performed in the single pass mode of operation due to reasons explained in Chapter II.D. The rest of the experiments are performed in the recirculating mode of operation.

Since the knowledge of the flow field is important for the interpretation of the stability results, an attempt is also made toward a comprehensive understanding of the flow field using the diagnostic technique and the quantitative technique mentioned above. A discussion of results is presented in this chapter. The results obtained by the two methods are compared and the differences are discussed. In addition some results obtained using the hydrogen bubble visualization technique are presented and discussed in Appendix C.

A. Flow Field Determination

The flow field is investigated in relation to the axial velocity distribution, the tangential velocity distribution and the entrance and exit flow conditions. Fejer et. al.[36] in

their investigation concluded that the flow field in a rotating duct can be divided into three regions: 1) an inlet region, in which reverse axial flow may occur near the tube wall, 2) a central region, in which the flow is relatively independent of axial position, and 3) an outlet region, where reverse axial flow may occur near the axis of the tube. These experimental results are strongly supported by the analytical investigation of Lavan et. al.[37]

1. Flow Visualization Using Dye Streaks

Soon after completion of the apparatus attempts were made to determine the flow field along the rotating pipe. Flow visualization using dye streaks introduced by probes was carried out. Three types of experiments were set up to answer the following three questions:

1) What is the entrance axial velocity distribution and what are the changes in that distribution as the flow proceeds downstream?

2) Where and under what conditions is the fluid in the pipe in solid body rotation?

3) To what extent, and under what conditions, does reversed flow exist in the entrance and exit regions of the rotating pipe?

The experiments related to the first two of these questions were conducted using the dye probes described in Chapter II.D. A different dye probe was used in the experiments related to the third question. This latter probe is a 1/4 inch inside diameter tygon tube connected to a pressurized dye container.

To study the axial velocity distribution, short dye streaks (about 1/2 inch long) are pulsed and observed as they propagate downstream along the pipe. This test is carried out at laminar flow conditions for the stationary pipe as well as for different tangential Reynolds numbers. It is found that the dye streak pulses propagate downstream at the same rate and thus remain at the same relative axial position to each other. The only exception is the dye streak in the vicinity of the wall (presumably in the boundary layer formed downstream of the entrance porous plug). Hence, it is concluded that within the range of the three inner dye streaks (about 2/3 of the diameter of the pipe) the axial velocity is almost uniform.

The most important results from the dye visualization are the ones relevant to the presence of solid body rotation. Since the probes are all located on the same angle of the pipe section, the streak lines should remain on a single radial line, in the case of solid body rotation, as they advance downstream. This yields a pattern that looks like a ribbon twisted along the axis of the pipe. If the flow is not in solid body rotation,

the streak lines will tend to be oriented at different angles as they propagate downstream, yielding a pattern of four streak lines which appear to be different sizes of concentric helical spirals of different pitches.

Performing the above observations, it is found that for a fixed axial Reynolds number, as the tangential Reynolds number is increased, the time required to achieve solid body rotation is increased. Furthermore, when solid body rotation is achieved, its region extends over the whole length of the pipe between the porous plugs. The flow is indeed essentially in solid body rotation for swirl ratios less than or equal to four as was predicted in Chapter II.A. When the swirl ratio is larger than approximately four, it is impossible to achieve solid body rotation, with the 2% dense plugs, even if the pipe has been rotating for a very long time. The time required to reach solid body rotation for swirl ratio of say three is found to be approximately ten minutes.

Since the presence of flow reversal is possible at the entrance and exit regions of the rotating pipe, (see Lavan et. al.[37] and Fejer et. al.[38]), these regions were investigated.

A number of experiments were performed by observing the dye streaks, injected through the four probes in the rotating pipe, and noting the direction of the dye propagation. In these experiments the axial Reynolds number was fixed and the

tangential Reynolds number was increased up to swirl ratios of approximately 20. These experiments were performed for different axial Reynolds numbers. No evidence of reversed flows along the rotating pipe between the two porous plugs was observed.

When the 1/4 inch tygon tube was placed against the center of the upstream side of the inlet porous plug and along its axis, and dye was injected, the following was observed: for relatively high swirl ratios, the dye enters the porous plug at the axis and returns in the opposite direction (toward the upstream of the main flow) in the vicinity of the wall. When dye was supplied at the exit plug from its downstream end the following was observed: for relatively high swirl ratios the dye enters the porous plug at the axis (toward the upstream end of the pipe) and returns in the main flow direction in the vicinity of the wall. When the dye probe is moved slightly downstream and away from the rotating pipe, the dye injected follows the main flow as it comes out of the probe, and hence one may conclude that the observed recirculation is not due to the velocity of the dye relative to the flow.

These results agree with the conclusions of the study by Lavan et. al.[37] that predicts regions of recirculation for large swirl ratios and indicate that, within the operating range of the present investigation, the recirculating regions at the inlet and exit of the rotating pipe are maintained inside the porous plugs.

2. Measurements Using Thermistor Probes

The experiments performed using the thermistor probes were mainly concerned with the axial velocity distribution. In addition, the conditions at which the flow remains in solid body rotation were also investigated at the section where the stability measurements were conducted.

Since the probe is mounted radially in the pipe and rotates with it, it should not sense any tangential velocities if the flow is in solid body rotation. Hence, if the flow is at a fixed axial Reynolds number and is in solid body rotation, the D.C. component of the probe output should remain constant even with changing tangential Reynolds numbers. The only restriction is the requirement that the axial velocity distribution should remain the same as the swirl ratio is increased. This restriction is satisfied for the range of swirl ratios less than four, where the tangential motion does not substantially affect the axial velocity profile (see Talbot,[39] Kavan et. al.[37] and Fejer et. al.[38]). This is true then for all radial positions where the sensing element in the probe can be located.

A series of experiments were performed for different fixed axial Reynolds numbers and increasing tangential Reynolds numbers. The D.C. component of the thermistor output was observed on both the digital voltmeter and the oscilloscope. The oscilloscope sweep for these experiments was maintained at a very low rate (1 sec/division). The same experiment

was repeated for different fixed tangential Reynolds numbers and increasing axial Reynolds numbers. It was observed in both sets of experiments that the output remains constant at swirl ratios less than approximately four. For swirl ratios larger than four, the digital voltmeter reading is periodically changing, while the output on the oscilloscope for these cases appears in the shape of a sinusoidal wave (see Fig. 10). The period of this output, measured on the oscilloscope, is found to correspond to the pipe rotation.

The preceding procedure was repeated for three different radial positions of the sensing element in the probe. Probe 2 and Probe 3, which were used in this study, gave identical results.

A series of experiments were also performed in connection with the axial velocity distribution at different axial eynolds numbers with the pipe being stationary. The experiments covered axial Reynolds numbers up to 7,000 in steps of 500. The probe was placed at eight different, equally spaced radial locations between the wall and the axis of the pipe, at an axial distance of approximately 19 pipe diameters downstream of the pipe entrance.

It was found, within the accuracy of the measurements, that the shape of the axial velocity profile remains essentially the same for the range of Reynolds numbers within the laminar

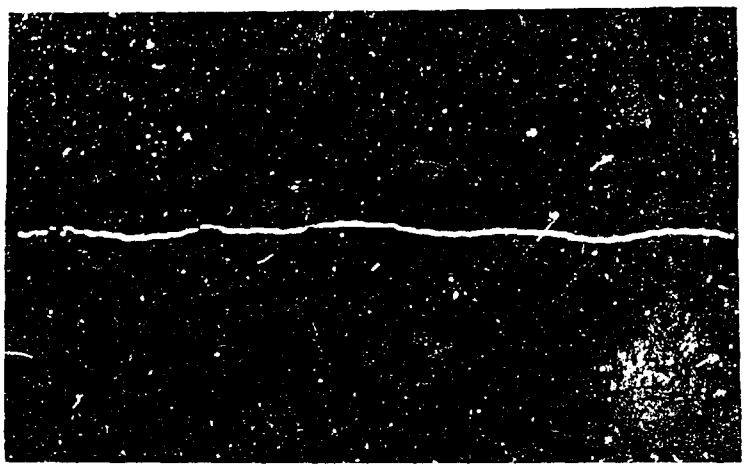

A. LAMINAR FLOW IN SOLID BODY ROTATION ($\Gamma < 4$)

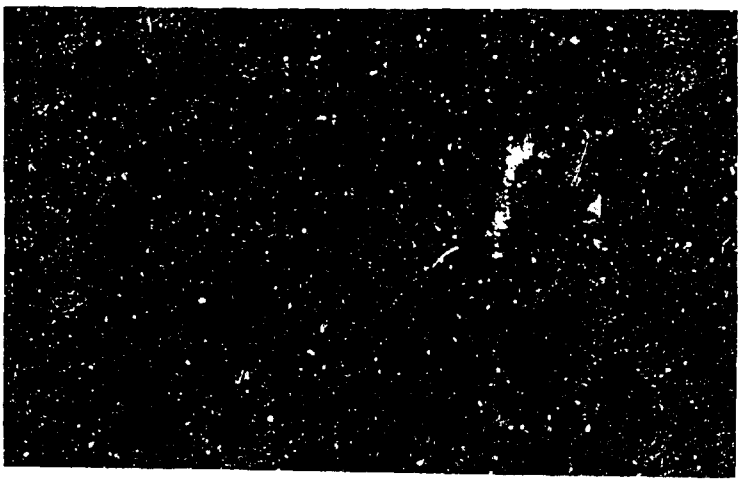

B. LAMINAR FLOW NOT IN SOLID BODY ROTATION ($\Gamma > 4$)

FIG. 10. OSCILLOSCOPE TRACES FOR DISCRIMINATION OF SOLID BODY ROTATION (SWEEP = 1 SEC/CM; SCALE = 1 MV/CM)

regime. As the flow changes from the laminar regime to the turbulent regime, the axial velocity profile changes and remains essentially the same for the whole range of axial Reynolds numbers within the turbulent regime. The laminar and turbulent axial velocity profiles are shown in Fig. 11.

B. Study of Stability

The study of the stability of flow in rotating pipes was performed in the present investigation by means of diagnostic and quantitative techniques. It is to be noted that the only difference in applying the two techniques is the position along the rotating pipe where the technique is used. The dye streak visualization technique was centered on a section about three pipe diameters downstream of the porous inlet plug, while the thermistor probe measurements were performed at a section about 19 pipe diameters downstream of the inlet. In both cases the emphasis was on the determination of the dependence of the transition from the laminar to the turbulent regime on the axial and tangential Reynolds number.

1. Flow Visualization Using Dye Streaks

Dye streaks are introduced by the dye probes into the flow field in order to determine the transition from laminar to turbulent regimes. These tests can be subgrouped in the following manner:

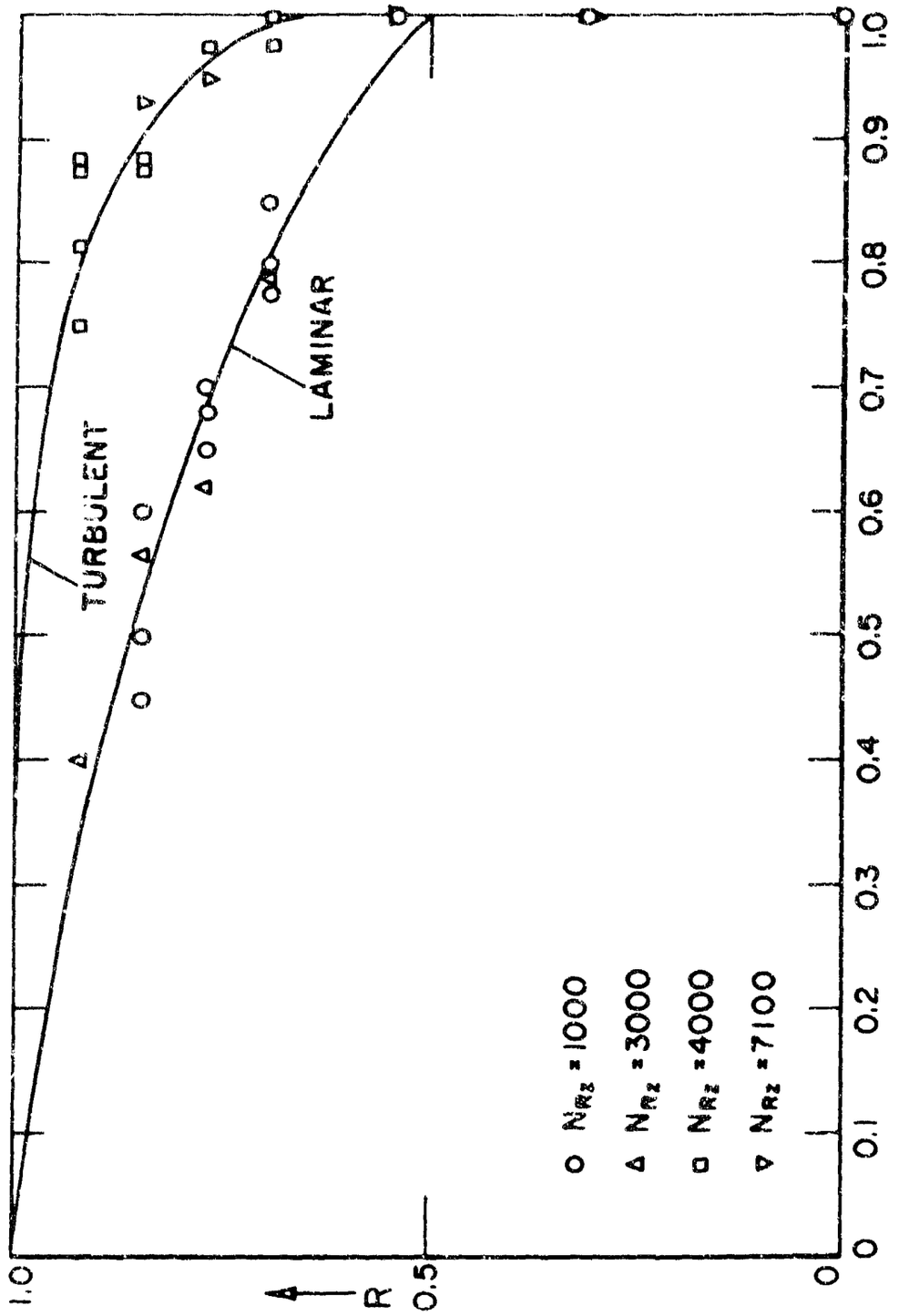

FIG. 11. LAMINAR AND TURBULENT MEAN AXIAL VELOCITY PROFILES.

1) Dye streak observations for non-rotating pipe with increasing axial Reynolds numbers.

2) Dye streak observations for different fixed axial Reynolds numbers with increasing tangential Reynolds numbers.

3) Dye streak observation for different fixed tangential Reynolds numbers with increasing axial Reynolds numbers.

The dye streak observations were performed in the same manner as those of the historical investigation of Reynolds,[1] in which he determined the transition from the laminar to the turbulent regime in circular pipes.

Photographs of the dye streaks for various axial Reynolds numbers with the pipe stationary ($N_{R\theta} = 0$) are shown in Fig. 12. At the low axial Reynolds numbers the dye streaks are undisturbed, indicating that the flow is laminar. As the axial Reynolds number is increased, the dye streaks become more and more disturbed and eventually break up, indicating a turbulent flow.

In Fig. 13 photographs of the dye streaks are presented for a fixed axial Reynolds number (one that is laminar with the pipe stationary) and increasing tangential Reynolds numbers. It is observed that the flow becomes turbulent as the tangential Reynolds number is increased. Observations at different fixed tangential Reynolds number (not shown) indicate that transition to turbulent flow occurs at a lower tangential Reynolds number when the axial Reynolds number is higher.

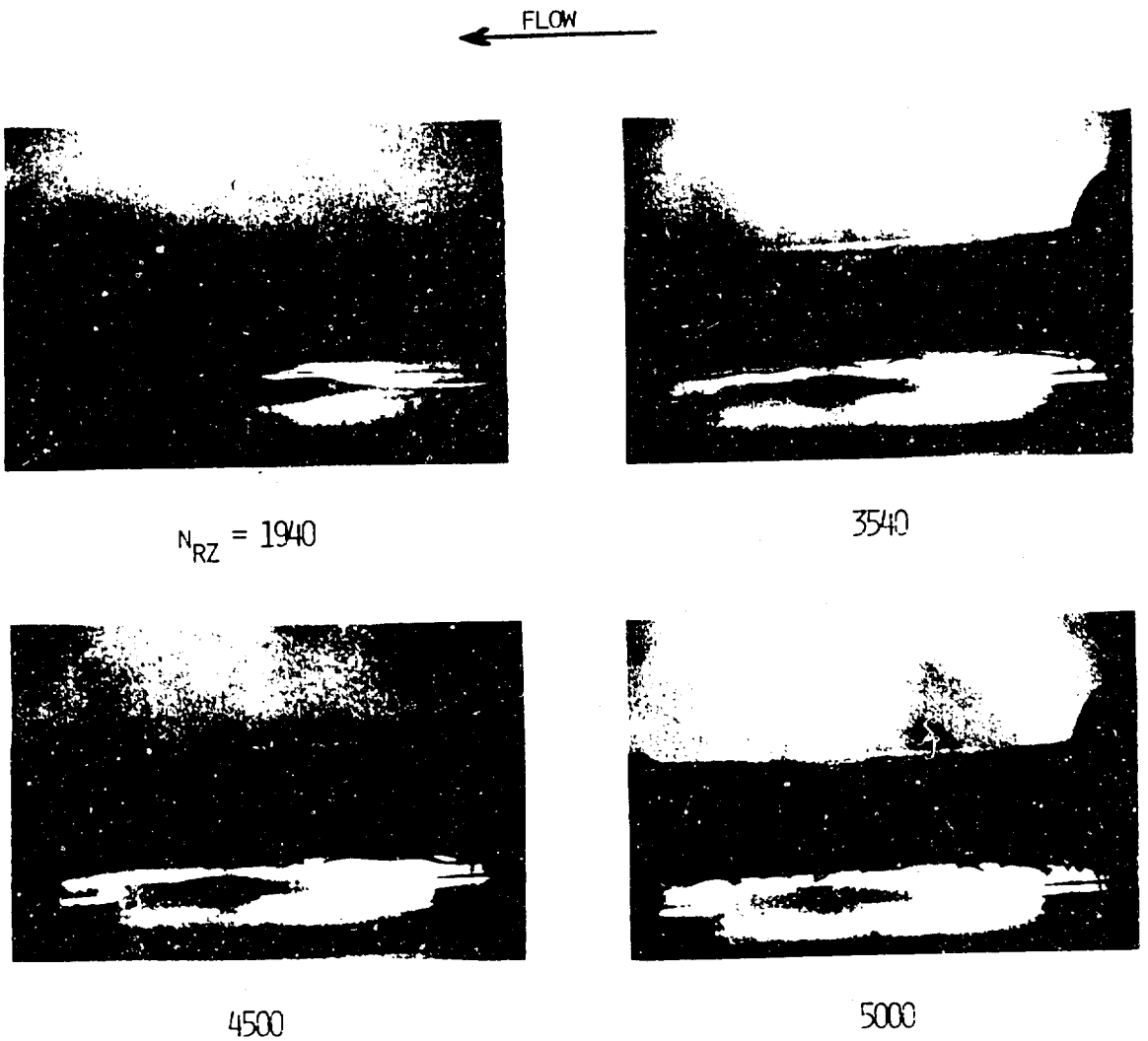

FIG. 12. DYE STREAKS FOR INCREASING AXIAL REYNOLDS NUMBERS WITH NO ROTATION ($N_{R\theta} = 0$)

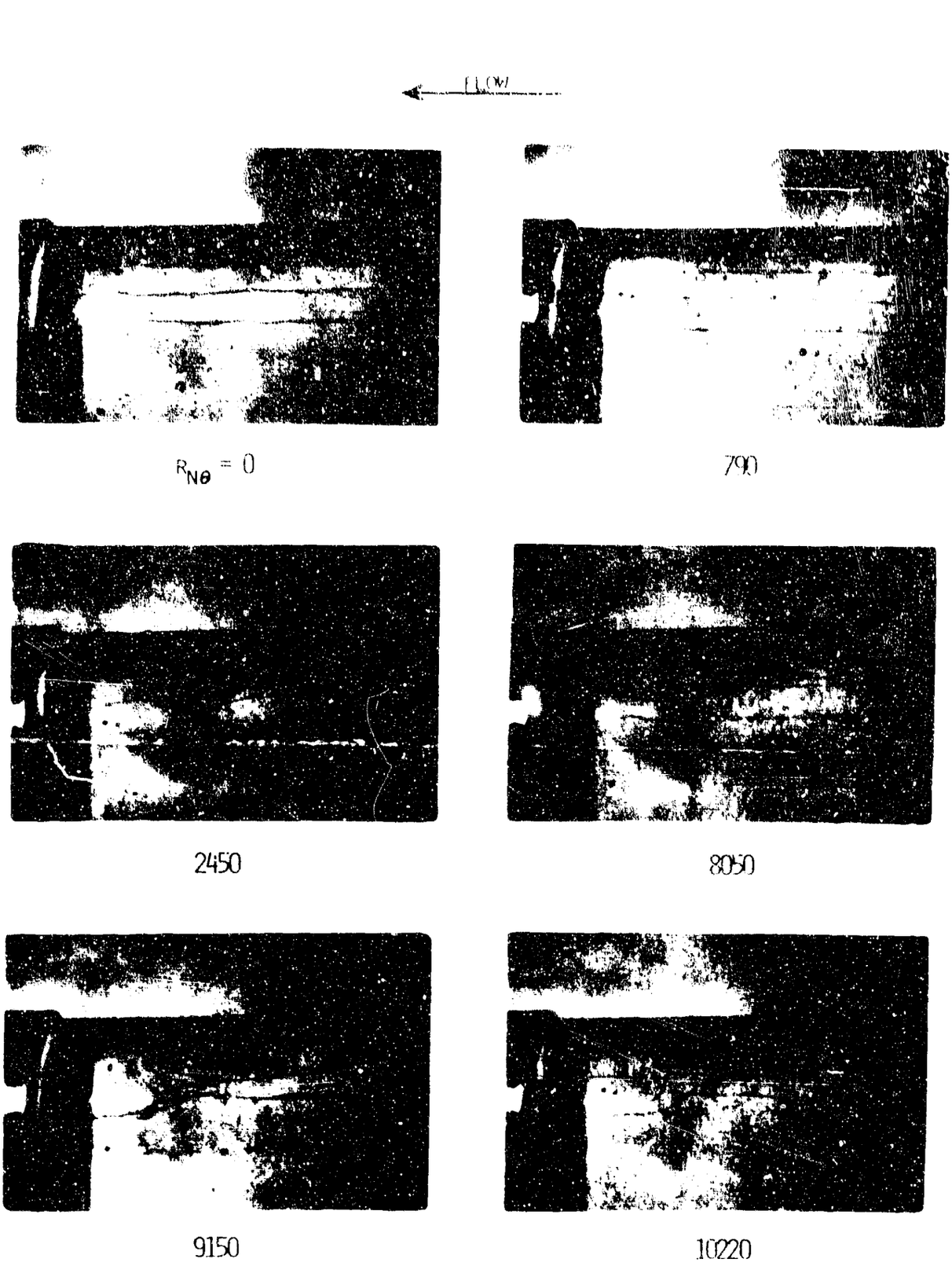

FIG. 13. DYE STREAKS FOR INCREASING TANGENTIAL REYNOLDS NUMBER AT A FIXED AXIAL REYNOLDS NUMBER ($N_{RZ} = 3300$)

The increasing tangential Reynolds number was also found not to change the turbulent regime to a laminar one for an axial Reynolds number yielding turbulent flow when the pipe is stationary. This result disagrees with the results obtained by White[34] and Cannon et. al.[35]

The dye streak photographs shown in Fig. 14 are for fixed tangential Reynolds number and increasing axial Reynolds number. Here it is observed that transition to turbulence occurs at lower values of the axial Reynolds number when the tangential Reynolds number is increased.

While studying the dye streaks as they change from the undisturbed to the disturbed patterns, indicating transition from the laminar to the turbulent regime, it was observed that the streaks revealed at first a regular wavy pattern (see Fig. 13 and Fig. 14) before amplifying and breaking into irregular patterns.

It was also found that the dye streak observations are much clearer and easier to interpret in those experiments using the fixed tangential Reynolds numbers and increasing axial Reynolds number than in those using fixed axial Reynolds numbers and increasing the tangential Reynolds number. This is due to a number of factors; the most important being the long time required to reach solid body rotation at high tangential Reynolds number. The observations of the dye streaks are summarized in Fig. 15, where a curve of transition from laminar

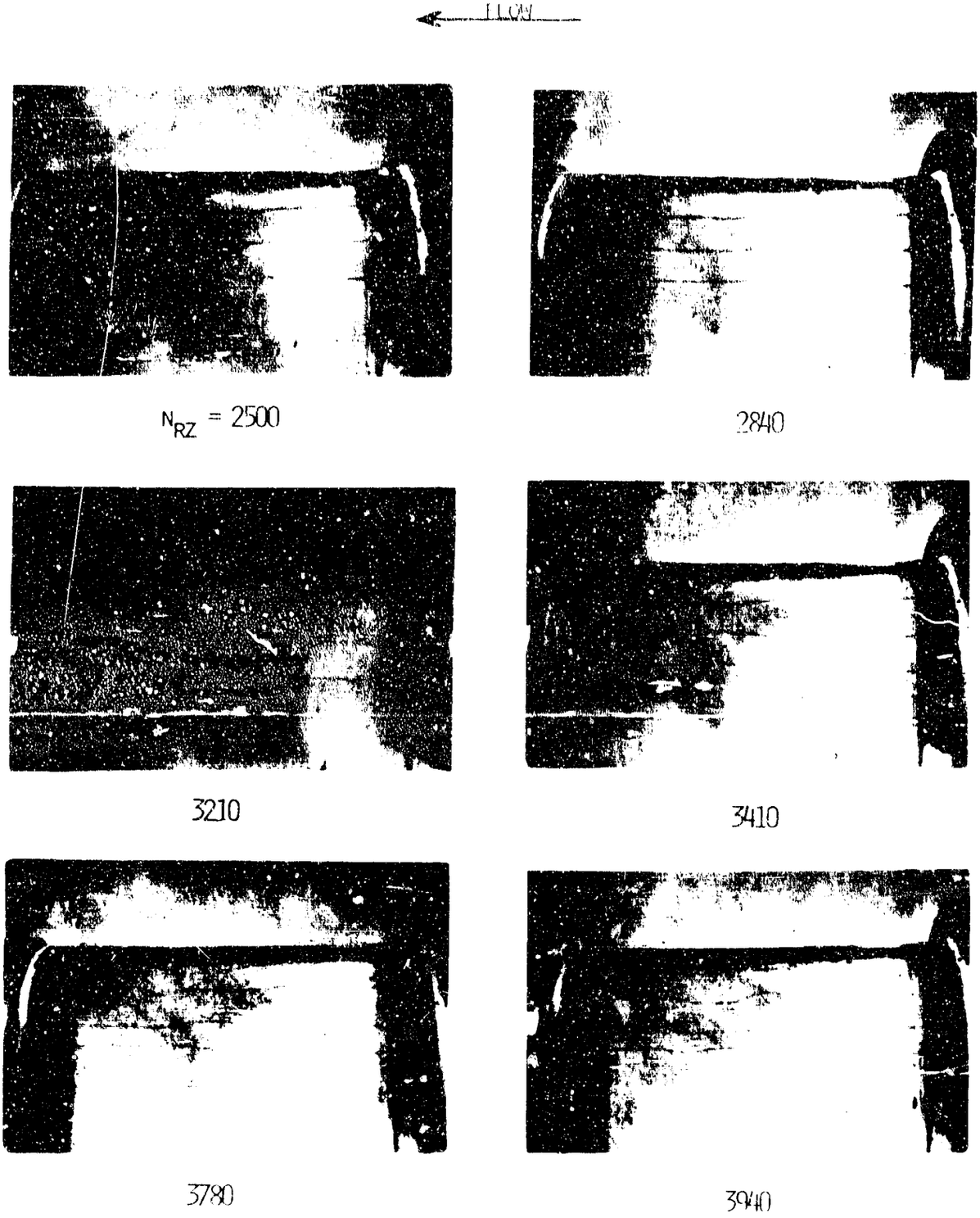

FIG. 14. DYE STREAKS FOR INCREASING AXIAL REYNOLDS NUMBER AT HIGH ROTATION ($N_{R\theta}$ = 6700)

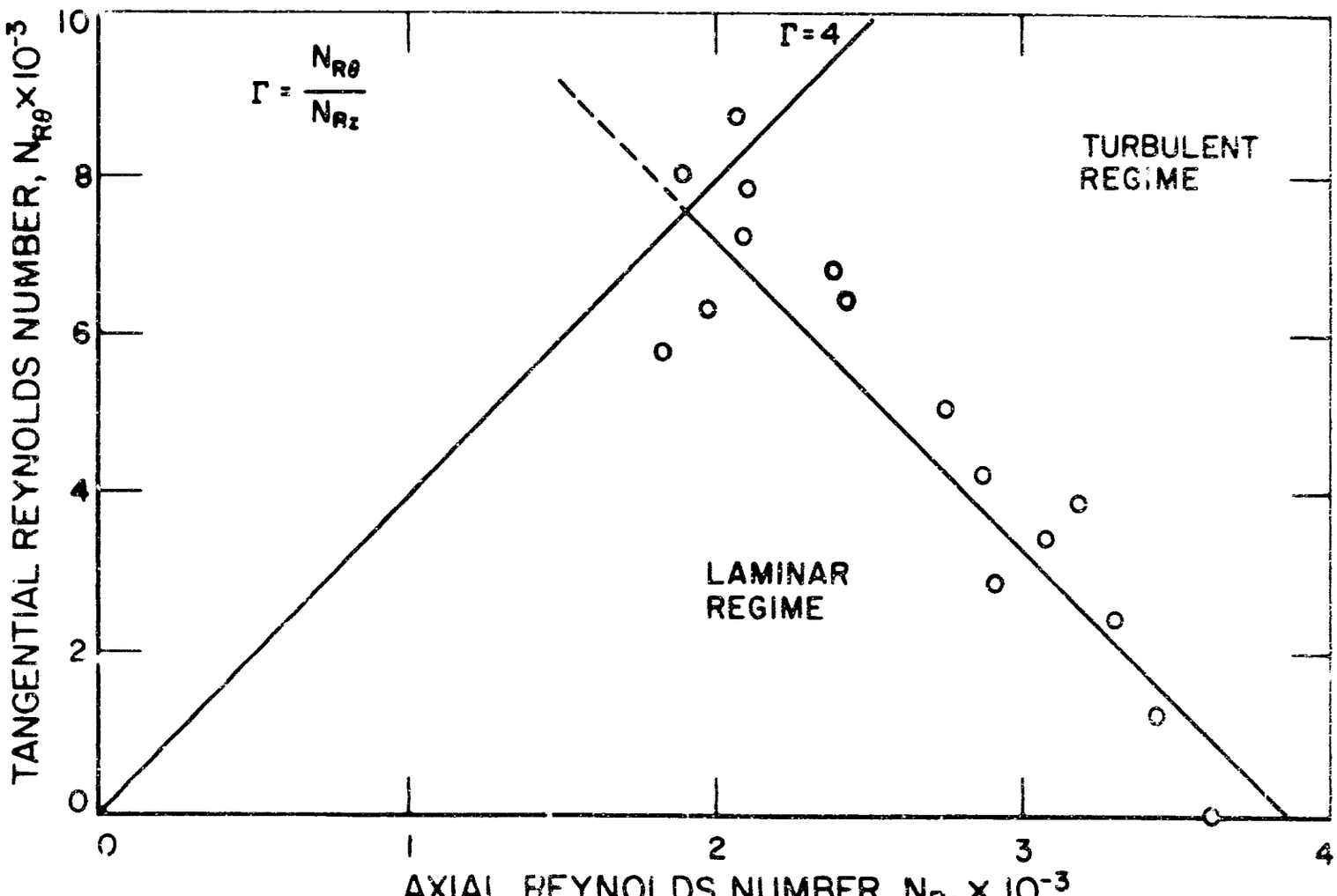

FIG. 15. LAMINAR-TURBULENT FLOW REGIMES IN ROTATING PIPE. DATA BASED ON DYE STREAKS OBSERVATION.

to turbulent regimes is shown as a function of axial and tangential Reynolds numbers.

2. Measurements Using Thermistor Probes

From the dye streak visualization stability data it was concluded that it is more convenient to use fixed tangential Reynolds number and increasing axial Reynolds numbers rather than using fixed axial Reynolds numbers and increasing the tangential Reynolds number. It should be also noted that the two approaches yield the same results (points on the same curve). Hence, the first method was the only one used in the hot-thermistor anemometry measurements.

Transition from laminar to turbulent regimes can be measured using sensing elements with a limited frequency response. This is possible since the spectrum of turbulent velocity fluctuations covers a wide frequency range. In addition, the amount of energy in the low frequency range is usually larger than that in the high frequency range. This explains that a typical turbulence spectrum has usually an overall negative slope (see, e.g., Hinze[40] and Schlichting[41]).

Thermistor Probes 1 and 4, which were used for the stability measurements, have maximum frequency responses of approximately five c.p.s. and ten c.p.s., respectively. Thus, it should be understood that the probes sense only the energy contained in the range of velocity fluctuations in the flow field, which is bounded by their maximum frequency response.

By monitoring the output of the probes on the oscilloscope and at the same time recording the RMS value of the A.C. component using a true RMS meter, adequate information about transition from the laminar to the turbulent regime was obtained. Typical oscilloscope traces at different flow conditions using different sweep rates are shown in Fig. 16.

The RMS values of the thermistor output as a function of axial Reynolds number were obtained at different fixed tangential Reynolds numbers. Two of these curves are shown in Fig. 17.

While obtaining these readings, pictures of the oscilloscope trace were taken. Two sets of these pictures are shown in Fig. 18, for the stationary pipe and for a tangential Reynolds number of 1735.

Studying the curves, it is concluded that the first straight line portion of the curve corresponds to the laminar regime, the second to the transition regime, and the third to the turbulent regime. These data are replotted in Fig. 19 to show the three regimes as a function of axial and tangential Reynolds numbers.

Similar information can also be deduced by studying the pictures in Fig. 18. It should be apparent from these pictures where transition from laminar to turbulent regimes starts and where it ends, for both the rotating and the non-rotating flow conditions. Some of the conclusions which are obvious from the pictures are:

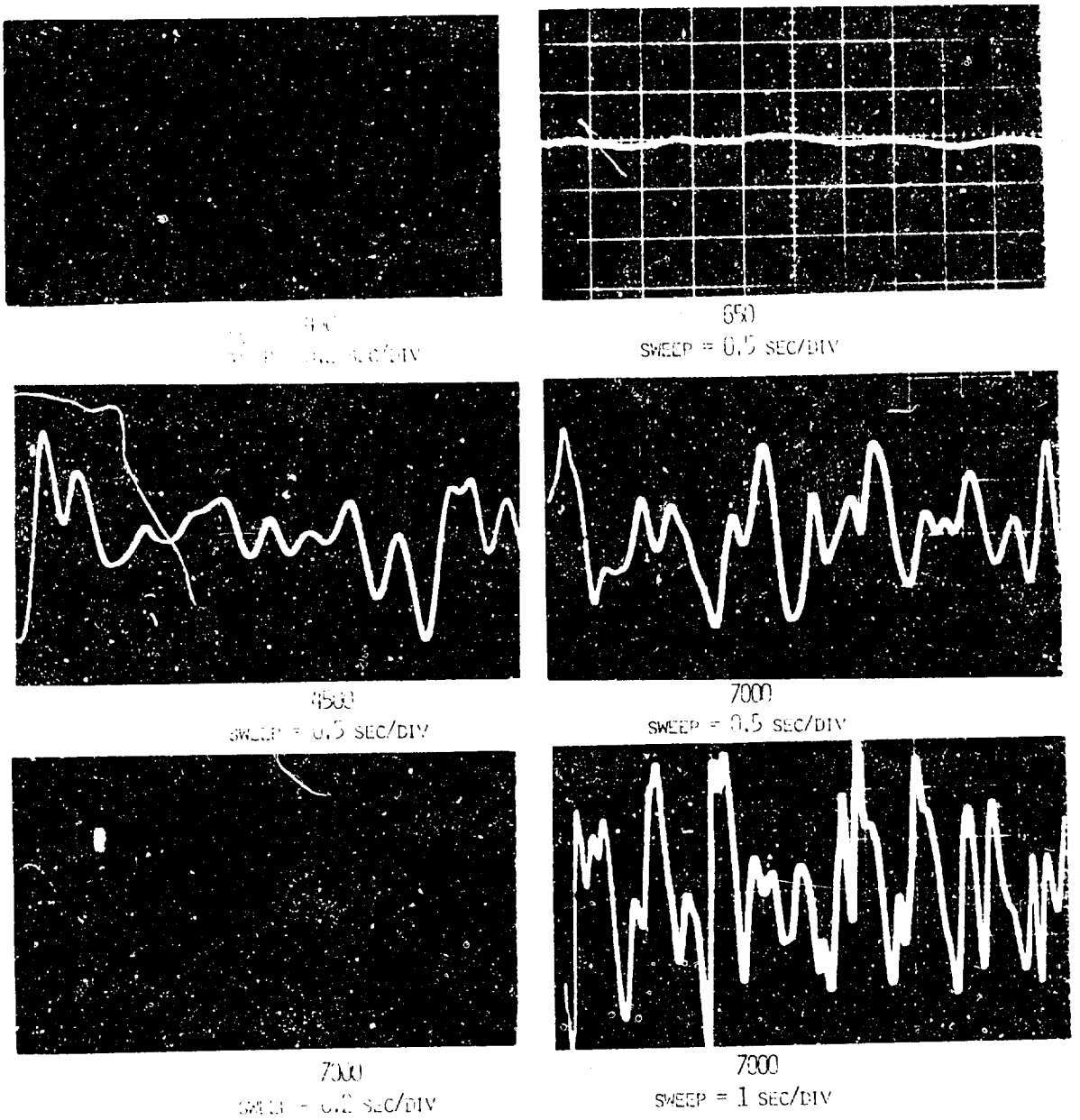

FIG. 16. OSCILLOSCOPE TRACES AT DIFFERENT AXIAL REYNOLDS NUMBERS WITH NO ROTATION (SCALE = 1 MV/DIV)

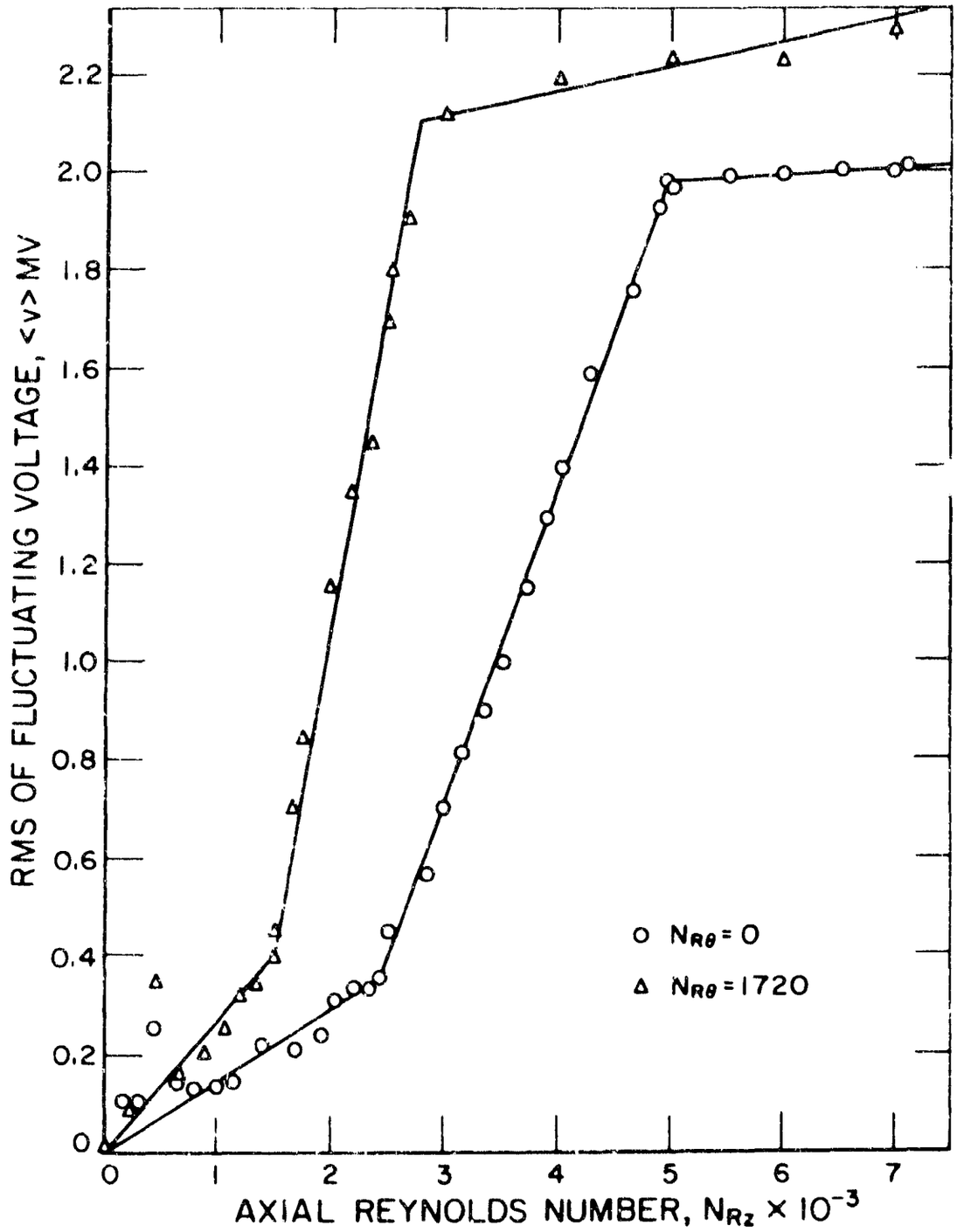

FIG. 17. RMS OF THERMISTOR OUTPUT AT INCREASING AXIAL REYNOLDS NUMBER FOR TWO FIXED TANGENTIAL REYNOLDS NUMBERS.

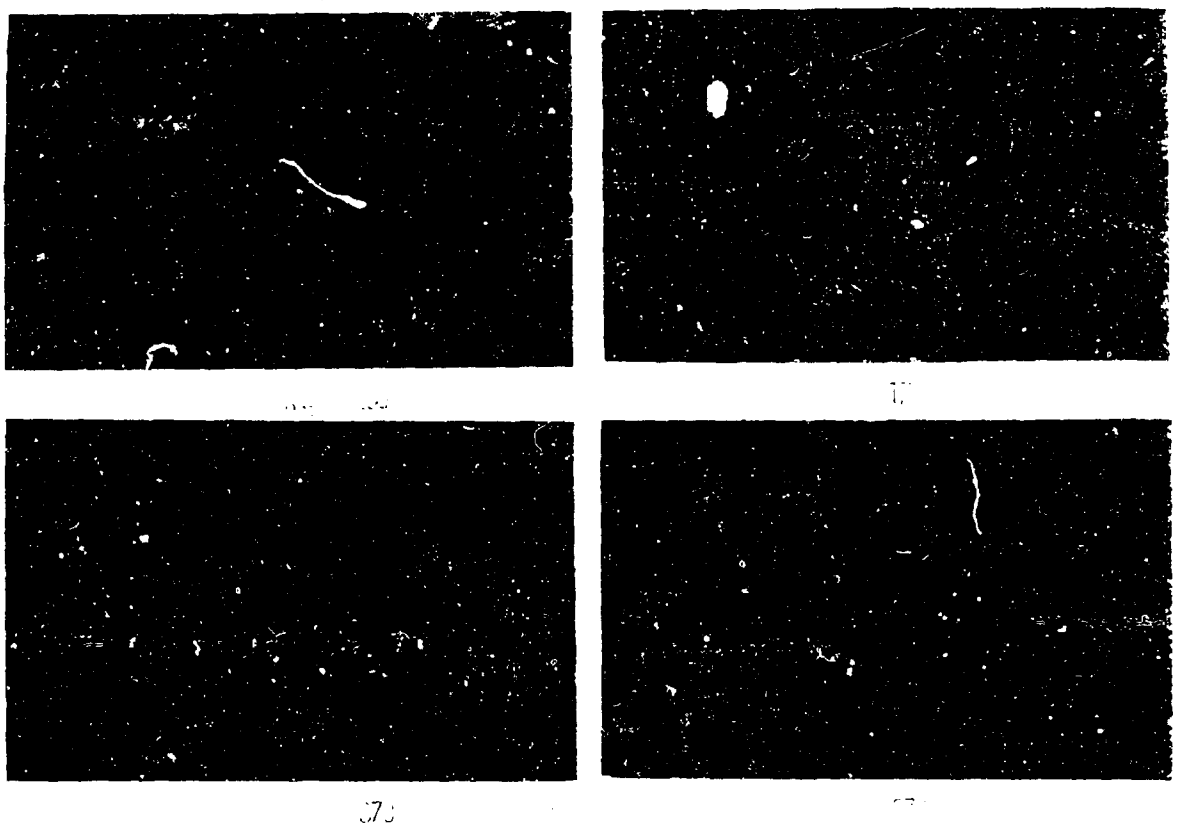

FIG. 18. OSCILLOSCOPE TRACES AT INCREASING AXIAL REYNOLDS NUMBER FOR TWO FIXED TANGENTIAL REYNOLDS NUMBERS

$N_{R\theta}$ = 1735 FOR LEFT COLUMN

$N_{R\theta}$ = 0 FOR RIGHT COLUMN

(SWEEP = 0.2 SEC/DIV; SCALE = 1 MV/DIV)

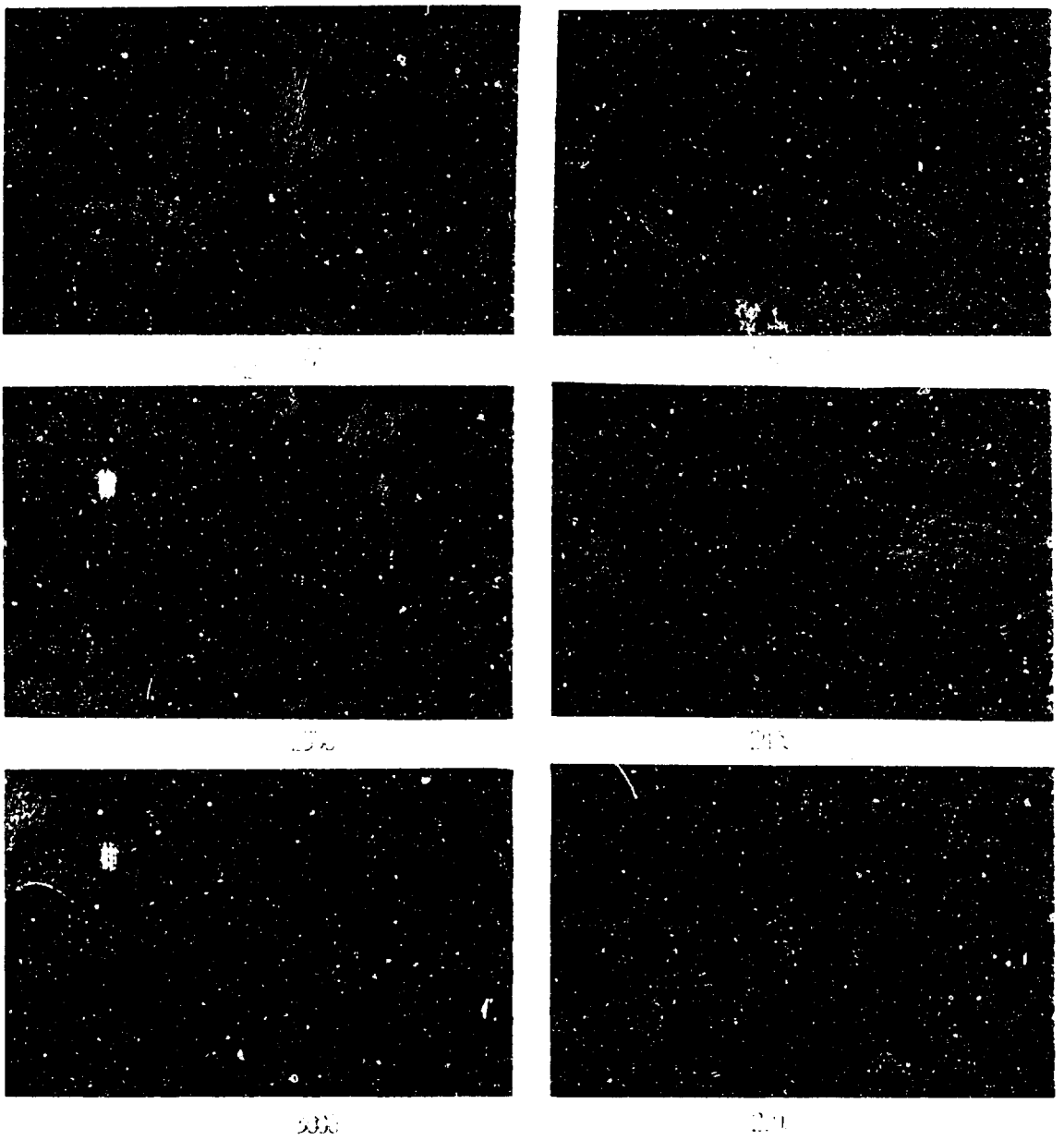

FIG. 18. (CONT'D)

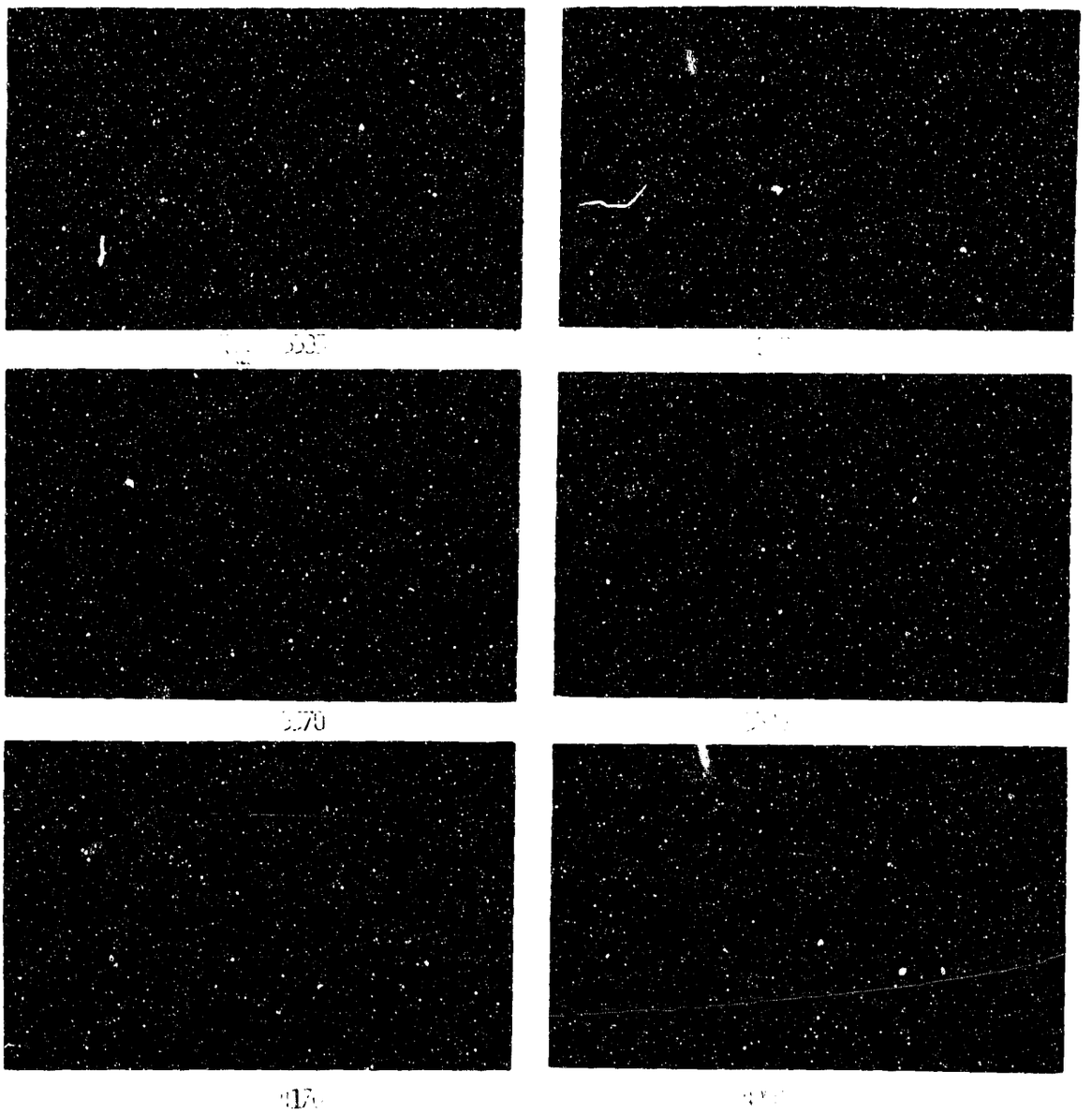

FIG. 18. (CONT'D)

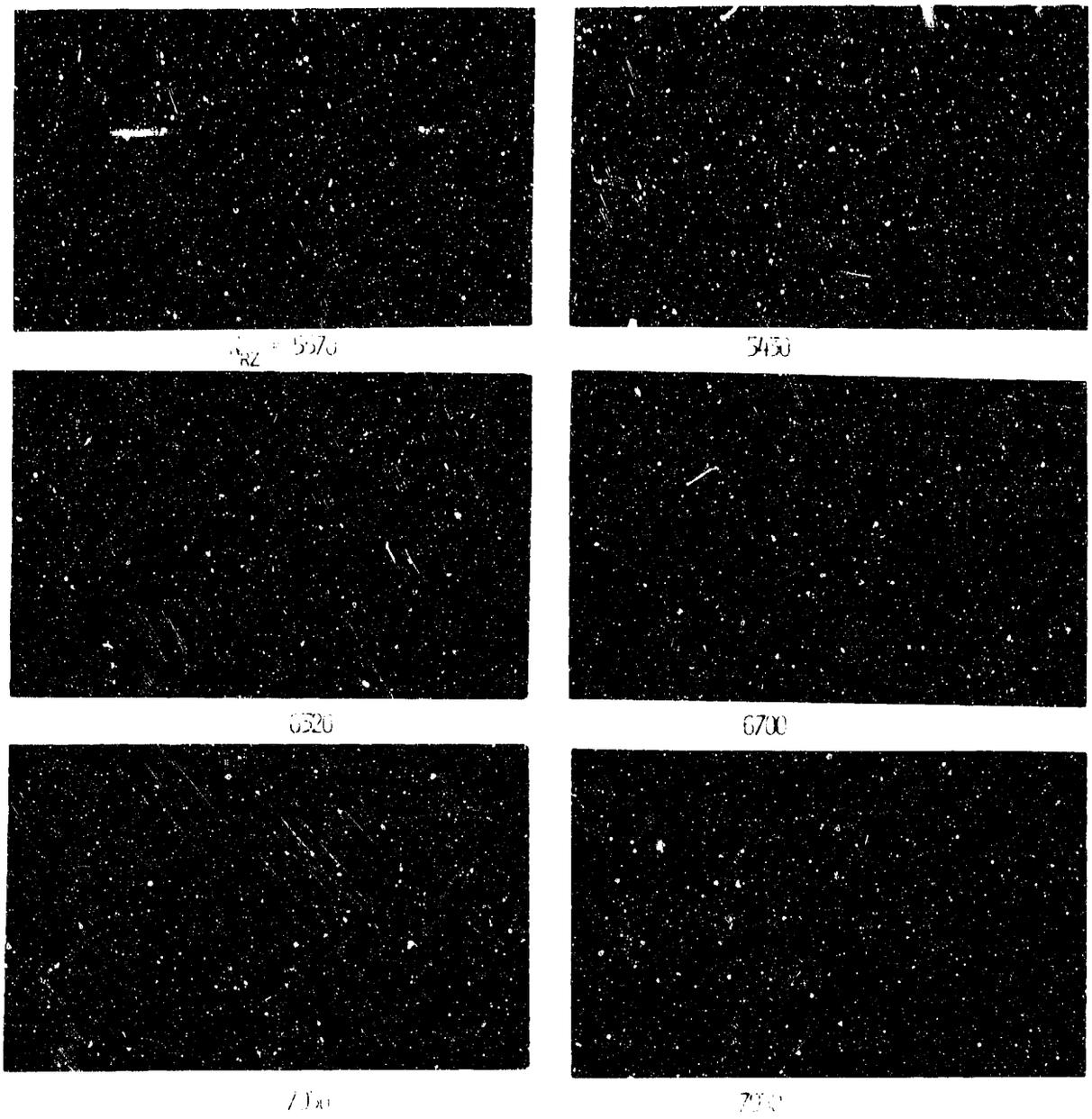

FIG. 18 (CONT'D)

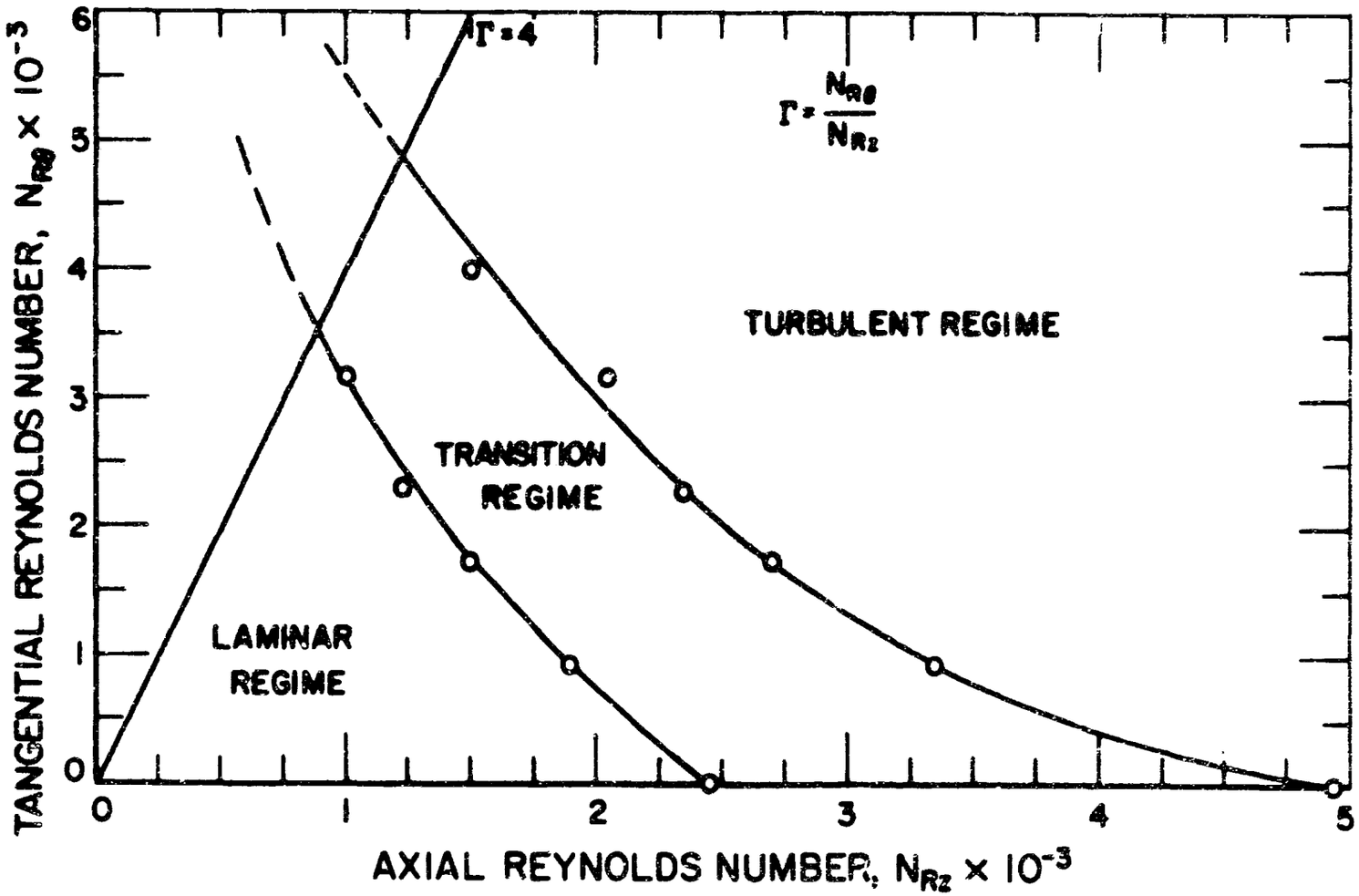

FIG. 19. LAMINAR-TRANSITION-TURBULENT FLOW REGIMES IN ROTATING PIPE, DATA BASED ON THERMISTOR MEASUREMENTS.

1) The pictures on the first page (of Fig. 18) indicate that both the rotating and non-rotating flows are in the laminar regime ($N_{Rz} < 1000$).

2) The pictures on the second page indicate that the rotating flow is in the transition regime while the non-rotating flow is still laminar ($1700 < N_{Rz} < 3000$).

3) The pictures on the third page indicate that the rotating flow is in the turbulent regime while the non-rotating flow is in the transition regime ($3200 < N_{Rz} < 4200$).

4) The pictures on the last page indicate that the rotating and non-rotating flows are in the turbulent regime ($N_{Rz} > 5500$).

All the hot-thermistor measurements leading to the curves presented here were performed with the sensing element of the probe located at the axis of the pipe. Similar information (not shown here) was also obtained for other radial locations of the sensing element (excluding the boundary layer). The results indicate only a small shift of the curves of Fig. 19 toward lower values of Reynolds numbers. It is therefore believed that the results obtained at the axis are adequate to describe the transition phenomenon.

From curves such as those shown in Fig. 17, it was observed that a high RMS value was measured at an axial Reynolds number of approximately 450, and it was found that this phenomenon is independent of the tangential Reynolds number. Further

investigation revealed a distinct frequency on the oscilloscope. The output signal under these conditions (N_{Rz} = 450) is shown in Fig. 16 revealing a frequency of approximately 6.5 c.p.s. The frequency was also measured using the octave band analyzer and the same result was obtained. No explanations are available at present for this observed phenomenon.

C. Discussion of Results

The results presented in this chapter are concerned with the flow field determination as well as investigation of the stability. Two different techniques were used to achieve the results; one is diagnostic and the other is quantitative. For the stability results the diagnostic approach is only used to indicate the trend of the stability of flow in rotating pipes and to confirm the results obtained by the quantitative approach. For mean flow measurement both approaches are of equal significance.

With regard to the flow field determination, several areas were investigated. One of these concerns the existence of reversed flow in the flow field. This area was investigated only by means of the diagnostic flow visualization technique and the results obtained were found to agree with the analytical investigation of Lavan et. al.[37] It is concluded from these results that the flow field in the rotating pipe between the porous plugs is free of reversed flow within the range of the results of the present investigation.

The results relevant to the tangential velocity profile, obtained by the two measurement techniques, are in agreement. It should be noted that the dye streak visualization technique covers the whole length of the pipe, while the hot-thermistor measurements are performed at only one section of the pipe (the location at which the stability measurements are performed). From these results it is concluded that the flow is in solid body rotation up to swirl ratios of approximately four.

The diagnostic technique does not contribute to the axial velocity profile measurements except by providing some support to the data provided by the quantitative technique. These results agree favorably with results from similar cases (laminar and turbulent velocity profiles for the entrance region of circular pipes) quoted by Prandtl et.al.[42], Schlichting[41] and Goldstein.[43] They also agree favorably with the results obtained using hydrogen bubbles which are presented in Appendix C.

The results of the diagnostic dye streak observations are presented here for two reasons. The first is to confirm the results obtained by the quantitative hot-thermistor anemometry technique since they both agree on the effect of rotation on the stability of flow in rotating pipes. The second is to present a comparable technique to the one used by White[34] and Cannon et.al.[35] in a similar investigation. The results in their investigation and the destabilizing effect of rotation on the stability of flow in rotating pipes as given in Fig. 15 are contradictory.

The results obtained by the two different techniques used in the present investigation (see Fig. 15 and Fig. 19) are not in complete agreement. This is believed to be due to the following reasons:

1) The porous plugs are known to introduce small scale eddies, due to shedding from the porous face of the plug. These eddies tend to affect the dye visualization data, since the dye streaks are being observed a small distance downstream of the plug. These eddies die out within a short axial distance due to viscous effects and hence will not affect the thermistor probe measurements. (The probe is located about 19 pipe diameters downstream of the upstream porous plug.)

2) Dye visualization experiments are performed in the single pass mode, in which stable flow rates cannot be maintained (see Chapter II.C.). The fluctuation of the flow rate is believed to affect the dye streak data. Hot-thermistor measurements are performed in the recirculating mode, in which stable flow rates are obtained.

Despite these discrepancies, the destabilizing effect of rotation can still be determined from the dye streak data. The opposite effect is concluded by the similar investigation of White[34] and Cannon et. al.[35] The results obtained using hydrogen bubbles and presented in Appendix C confirm the stability results obtained using dye streaks and thermistor anemometry.

The results obtained by the hot-thermistor measurements are believed to be accurate. It should be pointed out that they agree in trend with the results of the recent analytical investigations by Pedley[32] and Strohl.[33]

CHAPTER IV

CONCLUSION AND RECOMMENDATION

Solid body rotation is found to have a destabilizing effect on flow through pipes. The flow field investigated consists of solid body rotation superposed on an entrance type pipe flow profile. The destabilizing effect of rotation increased continuously with increasing swirl ratios in the range investigated. The results obtained (see Fig. 19) agree therefore in trend with results obtained analytically by Pedley[32] and Strohl[33] who investigated a fully developed axial profile at high swirl ratios. They found that in the limit of very high rotation the flow will be unstable for axial Reynolds numbers as low as 82.9. The present results suggest that the destabilizing effect due to solid body rotation may also hold for other axial velocity profiles and for the core of swirling flows in stationary ducts and free vortices. At the operating conditions of the present investigation solid body rotation was maintained up to swirl ratios of four; hence, this was the upper limit of the swirl ratios investigated. Two different measurement approaches are used; one is diagnostic and the other is quantitative. The diagnostic is the flow visualization technique using dye streaks and the quantitative is the hot-thermistor anemometry technique. Both approaches yield similar results for the breakdown of the laminar flow. A limited investigation of the flow field and the stability of the flow was also conducted using the hydrogen bubble visualization technique (see Appendix C). The results obtained agree favorably with the results obtained using the two other measurement approaches.

White[34] and Cannon et. al.[35] investigated experimentally the effect of rotation on the stability of flow in pipes and concluded that rotation is stabilizing. The results obtained in the present investigation contradict their conclusions. It is believed that the results obtained by White are strongly influenced by reversed flow components that would indeed exist at the high swirl ratios used in his investigation (see Lavan et. al.[37]). The results of Cannon et. al.[35] are subject to a similar criticism, since they observed a core region in their pipe that was stationary while the pipe was rotating.

The present investigation indicates a possible new mechanism of confined flow instability that takes place at lower Reynolds numbers than previously believed possible. This conclusion is supported by the recent analytical works of Howard et. al.[24], Ludwieg,[26,27] Kiessling,[29] Pedley,[31,32] Strohl[33] and Joseph et. al.[13] In view of the fundamental aspect of this work, it is therefore suggested to continue and extend the investigation. The main objectives of the extension of the present study are:

1) To create predictable axial velocity profiles and to measure them precisely.

2) To generate higher swirl ratios while maintaining the desired axial flow profiles unchanged.

3) To carefully analyze the disturbances in order to compare them to the analytical predictions and to clearly identify the structure of the disturbed flow.

4) To increase precision and accuracy in all phases.

In an attempt to meet these objectives, two better and more advanced flow visualization techniques for mean flow measurements are presently considered; hydrogen bubbles and thymal blue. Hydrogen bubbles have been successfully used by Lennemann et. al.[44] in moderately rotating systems for quantitative diagnostics. Baker[45] introduced a visual measurement technique for small fluid velocities using thymal blue (thymolsulphonephthalein). The thymal blue is simple to use and since it remains in an ion solution density difference and centrifugal effects characteristic of hydrogen bubble techniques are absent here.

In order to directly observe the wave patterns calculated by Pedley[32] and Strohl,[33] a visualization technique utilizing aluminum flakes is suggested. Ludwieg[30] successfully used such a technique to visualize the wave patterns in a similar investigation. This technique may however, introduce some problems with the porous plugs.

Presently the use of more dense porous plugs is being investigated. Such a modification may permit the extension of the present investigation to higher values of swirl ratio. Plugs made of 20% dense material are currently being investigated.

In order to create experimentally a fully developed axial profile that will permit comparison with the investigations of Pedley[32] and Strohl,[33] two ideas are proposed. Pedley's[31,32]

analysis is valid for the flow in an annulus with solid body rotation at high swirl ratios. Thus, by introducing an inner cylinder in the apparatus that rotates with the outer pipe, one can conveniently investigate such a flow. If the gap between the pipe and cylinder is of sufficiently small size, the flow in the annulus will be fully developed within the length of the apparatus.

The second possible method is to use contoured porous plugs in order to obtain fully developed Hagen-Poiseuille flow. Such an approach requires an extensive amount of work in investigating porous media and shaping the porous plugs.

The use of glycerin as a working fluid is also under consideration. This would permit the use of more sensitive measuring elements, since the mean flow velocities would be higher for the same range of axial Reynolds numbers. This would also make possible investigations at lower axial and tangential Reynolds numbers.

APPENDIX A

POROUS MEDIA

The mathematical model that leads to Darcy's law for flow through porous media neglects inertia effects and considers a multiplicity of identical cylindrical passages through the porous medium.

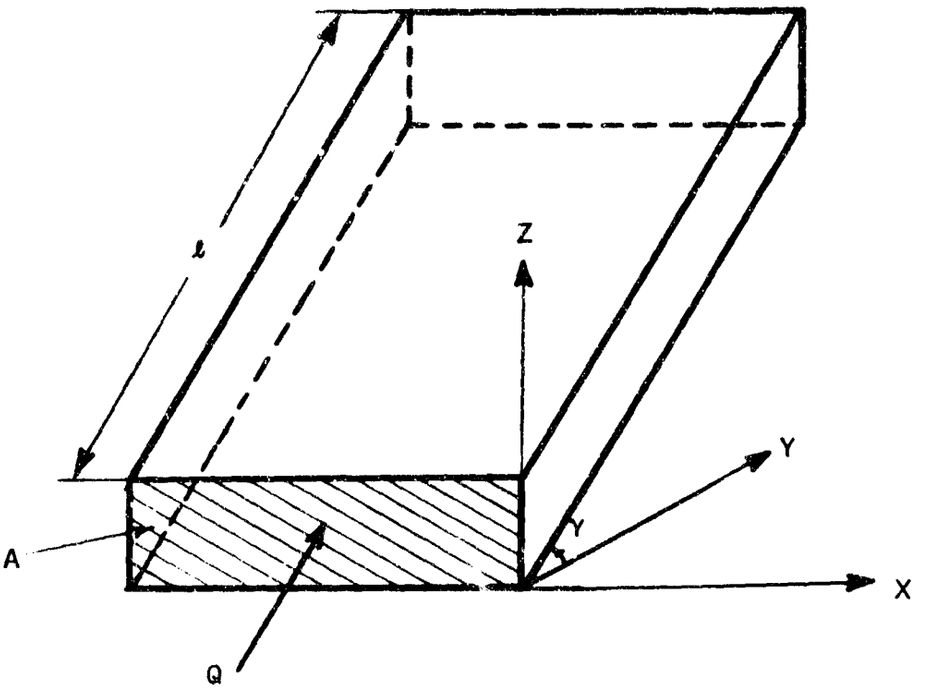

FIG. 20 MODEL OF POROUS MEDIA TO WHICH DARCY'S LAW IS APPLIED

Darcy's law applied to a porous volume element as shown in Fig. 20 yields (see e.g., Streeter[46])

$$Q = -\frac{KA}{\mu}\left[\frac{dP}{d\ell} + \rho g \sin\gamma\right] \qquad A.1$$

where Q is the volumetric flow rate and $dP/d\ell$ is the static pressure gradient in the direction of flow. This can be generalized to be represented in terms of velocity components,

$$V_x = -\frac{K}{\mu}\frac{\partial P}{\partial x} \qquad A.2a$$

$$V_y = -\frac{K}{\mu}\frac{\partial P}{\partial y} \qquad A.2b$$

$$V_z = -\frac{K}{\mu}\left[\frac{\partial P}{\partial z} + \rho g\right] \qquad A.2c$$

where V_x, V_y and V_z are velocity components along x,y and z and K is the permeability of the porous material.

The law thus shows that the pressure drop across a porous medium is proportional to the flow velocity. Darcy's law is applicable to porous media that do not consist of identical cylindrical passages, as long as the Reynolds number based on the effective particle diameter does not exceed unity. (The effective particle diameter is the dimension of the basic element in the porous material structure.) When this Reynolds number exceeds unity, the inertia effects become non-negligible and Darcy's law is no longer valid.

For the porous material used in the present investigation, the Reynolds number based on the effective particle diameter is found to be much larger than unity.

Arthur,[47] Bernicker[48] and Hill[49] present a more general approach that is applicable to this situation. In general, one may assume that a fluid (either compressible or incompressible) flowing through a porous medium encounters two kinds of resistance. They are:

1. Pressure drop across the porous medium due to the action of shear stress. This can be expressed in the form,

$$-\frac{dP}{dz} = \alpha \mu W \qquad A.3$$

where α is the coefficient of shear resistance.

2. A flow loss which is believed to be associated with sudden expansions and contractions along the flow passages and with the inertial effect at the turns and bends of the channels. This source of losses is not completely understood. It is usually expressed in the form,

$$-\frac{dP}{dz} = \beta \rho W^2 \qquad A.4$$

where β is the coefficient of inertial and compressible effects.

By combining these two pressure loss terms, the following general expression results:

$$-\frac{dP}{dz} = \alpha \mu W + \beta \rho W^2 \qquad A.5$$

This expression can be rewritten in the form,

$$-\rho \frac{dP}{dz} = \alpha \mu G \left[1 + \lambda \frac{G}{\mu}\right] \qquad A.6$$

where λ is called the friction length and is equal to $\frac{\beta}{\alpha}$, G is the mass flow rate per unit frontal area and is equal to ρW. One should note that within the present context α and λ define completely the permeability of a porous material independently of the flowing fluid. Normally α and λ (or α and β) as well as other properties are published by the manufacturers of the porous material.

Since the friction length λ, is of length units, we define a Reynolds number

$$N_{R\lambda} = \frac{\lambda W}{\nu}$$

The general equation for the pressure drop across a porous medium can therefore be expressed in the form

$$-\psi^2 \frac{dP}{dz} = N_{R\lambda} (1 + N_{R\lambda}) \qquad A.7$$

where

$$\psi^2 = \frac{\beta}{\rho \alpha^2 \nu^2}$$

For an incompressible fluid passing through a given porous material, ψ^2 is constant.

By comparing equations (A.5) and (A.7) it can be shown that:

a) For $N_{R\lambda} \ll 1$ the viscous resistance coefficient (α) determines the pressure drop, i.e., the pressure drop across the porous media is proportional the the flow velocity.

b) For $N_{R\lambda} \gg 1$ the coefficient of inertial and compressible effects (β) determines the pressure drop, i.e., the pressure drop across the porous media is proportional to the square of the flow velocity.

For the porous material used in the present investigation neither α nor λ are available from the manufacturers; thus, an experimental determination was made. The results are shown in Fig. 21, where the pressure drop across one-inch of the porous material is plotted versus the flow velocity on a logarithmic scale. The range of flow velocities corresponds to the range of axial Reynolds numbers from 0 to 5,000. The equation fitted to this curve is

$$\Delta P = CW^2 + B$$

$$= C'N_{Rz}^{\ 2} + B \qquad \text{A.8}$$

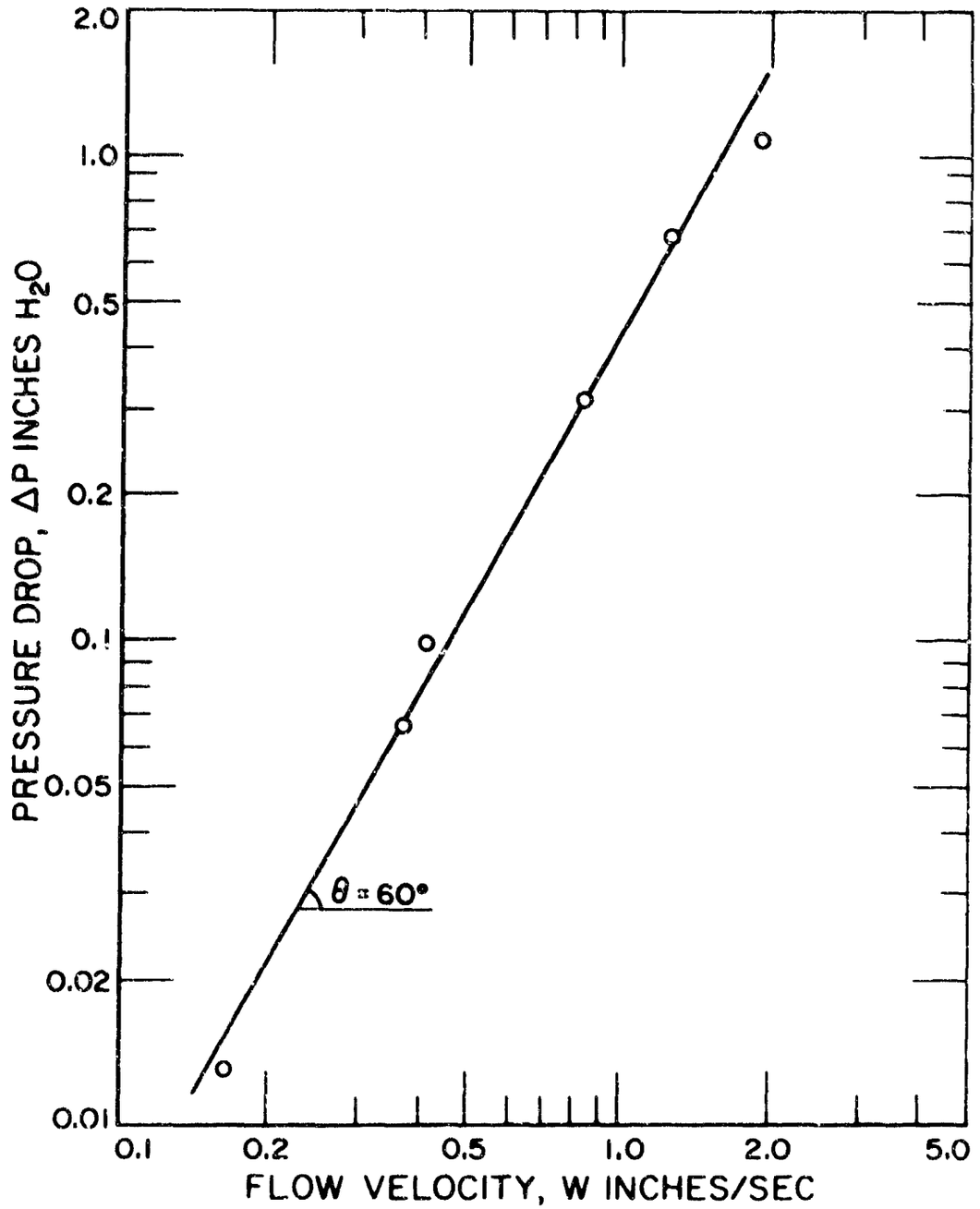

FIG. 21. PRESSURE DROP ACROSS ONE-INCH OF POROUS MATERIAL VERSUS FLOW VELOCITY.

where

$$C' = 3.66 \times 10^{-7} \text{ lb/ft}^2$$

and

$$B = 0.0293 \text{ lb/ft}^2$$

This result shows that the pressure drop across the porous material is proportional to the square of the velocity. This leads to the conclusion that, within our operating range, $N_{R\lambda}$ for the material used, is always larger than unity. This result could have been easily reached if the properties of this material would have been known a priori.

Assuming solid body rotation in the flow field, the radial pressure difference can be expressed in the form

$$\Delta P_r = \frac{\rho V^2}{2} = \frac{\mu^2}{2\rho D^2} N_{R\theta}^2 \qquad A.9$$

where D is the pipe inside diameter and V is the tangential velocity at this diameter. The axial pressure drop is

$$\Delta P_z = (\Delta P - B) = C' N_{Rz}^2 \qquad A.10$$

Dividing the two expressions we obtain

$$\frac{\Delta P_r}{\Delta P_z} = \frac{\mu^2}{2\rho D^2 C'} \Gamma^2 \qquad A.11$$

where

$$\Gamma = \frac{N_{R\theta}}{N_{Rz}}$$

For water flowing across one-inch of the porous material at room temperature, and with the outside diameter of the plug equal to 3-1/4 inches, the above expression reduces to

$$\frac{\Delta P_r}{\Delta P_z} \doteq 0.004 \quad \Gamma^2 \qquad \text{A.12}$$

By using this simple relation, the range in which the porous plug imparts solid body rotation to the fluid can be estimated. (See Chapter II.A). The comparison with experimental results is discussed in Chapter III.A.

APPENDIX B

HOT-THERMISTOR ANEMOMETRY

Thermistors have been investigated in the last ten years for their potential application as sensing elements. These investigations are mainly concerned with their properties, calibration and the possible areas of use. Thermistors are oxide semi-conductors with high negative temperature coefficients of electrical resistance (usually some combination of di-valent and tri-valent oxides such as CuO, NiO on one side and Mn_2O_3 and CO_2O_3 on the other side). Lumley,[50] Lane et. al.[51] and several other investigators contributed substantially to these investigations. Pertinent information is also published by the major thermistor manufacturers. However, few publications deal with the use of thermistors in fluid mechanics studies. This Appendix attempts to present a survey of thermistors and their technology; electronic circuitry, calibration procedure, and frequency response measurements, in particular, are discussed.

The two most common working fluids used in the fluid-mechanical experimental investigations are water and air. The differences between the two fluids which strongly affect the choice of the sensing element used are:

1. Typical velocities encountered in air tend to be much higher than those occurring in water.
2. Water tends to contain more impurities than air since many foreign particles have very nearly the same density and are, therefore, more difficult to remove.
3. The electrical conductivity of water is much higher than that of air.

For the above reasons, hot-wire anemometry, although very successfully used in air, is not commonly used in water. Instead the most frequently used sensing elements in water, and other liquids, are hot-film probes. Some of the hot-film probe materials are platinum or platinum alloys.

The principle of operation of both hot-thermistor and hot-film sensing elements is similar. If the sensing element is immersed in a still fluid and a heating current is supplied, it reaches thermal equilibrium with its environment when the internal heat generation rate is equal to the heat transfer rate by natural convection to the surrounding fluid. When the fluid is in motion, the sensing element temperature will drop, owing to the higher heat transfer rate by forced convection (the amount of drop being related to the fluid velocity). This drop in temperature will cause a change in the resistance of the sensing element.

The above introductory remarks lead to the conclusion that a choice between hot-film anemometry and hot-thermistor anemometry has to be made. Lumley,[50] in his investigation, presents a thorough comparison between the two types of sensing elements.

Lumley[50] concludes from his investigation that thermistors offer in water the possibility of spatial resolution and noise levels that are better by an order of magnitude than those obtainable with platinum film probes. This is due to their large resistivity and temperature coefficient of electrical resistivity, which are an order of magnitude larger than platinum. The resistivity as a function of temperature (T) has been experimentally found to be

$$R = R_{\infty} e^{T_o/T} \qquad B.1$$

where T_o is in the order of $2000^{o}K$ to $5000^{o}K$ and R_{∞} varies from one ohm to 75 megohms.

In addition to the above advantages, thermistors have lower density and smaller thermal conductivity than platinum. These properties have different implications; one is the need to insulate the probes. The most important consequence is the limitation of frequency response. An attempt to overcome this limitation using film deposition is presently in a development stage (see, e.g., Lumley[50]). This property though does not limit

their use in sensing transition from laminar to turbulent regimes. The probe usually consists of a thermistor bead mounted on a short support, and the bead is encapsulated in some insultaing material, such as glass. The probes are also rugged, and their high electrical resistivity permits the use of simple electronics.

Lane et. al.[51] introduced hot-thermistor anemometry for low velocity flow measurements. A method of calibrating the probes is explained in their work and the water temperature effect is also investigated. They concluded that hot-thermistor anemometry may be used to measure steady-state and transient velocities in the range from 0.1 to 6 inches per second, and that individual probe calibration is required. Except for measuring the response to step velocity changes, no attempt to measure frequency responses is reported.

Rotating systems introduce an additional problem in the use of sensing elements like hot-films or thermistors. In order to communicate the electric signals between the sensing element and the other anemometry components, one may use brushes and slip rings. Since the brushes and slip rings introduce noise, which is usually of a relatively high frequency, filtering is required. The large resistance of the sensing element makes the filtering easier and requires less expensive brushes and slip rings.

Based on the above discussion, hot-thermistor anemometry is chosen for the quantitative measurements in the present investigation. The probes are to be operated in the constant current mode, rather than the constant temperature mode, to achieve a higher sensitivity to velocity fluctuation and to reduce the cost of the electronic circuitry.

The different components forming the constant current hot-thermistor anemometer unit used are shown in Fig. 22. The 24-volt D.C. supply consists of two 12-volt medium-sized car batteries connected in series. The capacitance shown forms an R-C filter for suppressing the noise from the slip rings and brushes. The value of the resistance R used, is 4K ohm for the stability measurements, and 48K ohm for the flow field measurement. The reason for this is explained later in this Appendix.

Four different types of thermistor probes are used; the technical specifications of each are:

Probe 1. A GE thermistor (Cat. 81B 202) with the thermistor bead of 0.043 inch maximum diameter encapsulated in homemade insulation made of epoxy. (R_o = 2000 ohms)

Probe 2. A GE thermistor (Cat. 81G 202) with the thermistor bead encapsulated in a glass rod of 0.100 inch maximum diameter. (R_o = 2000 ohms)

Probe 3. A VECO thermistor probe (Cat. P32A129) with the thermistor bead encapsulated in a glass rod of 0.060 inch maximum diameter. (R_o = 2000 ohms)

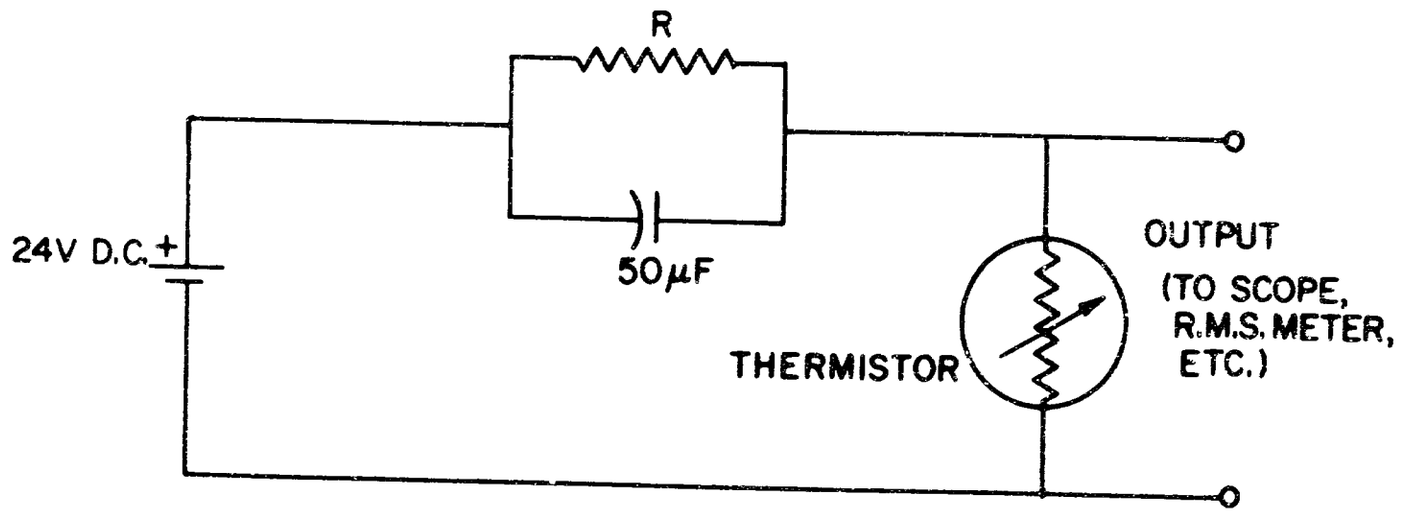

FIG. 22. CONSTANT CURRENT HOT-THERMISTOR ANEMOMETER UNIT.

Probe 4. A VECO thermistor probe (Cat. AZ31A70) with the thermistor bead encapsulated in a glass rod of 0.020 inch maximum diameter. (R_o = 1000 ohms)

All four probes are mounted at the ends of stainless steel tubing of diameters ranging from 1/16 to 1/8 inch. The thermistor connecting leads pass through the stainless steel tube. The probes are mounted inside teflon seals inserted in the wall of the pipe. The connecting leads of the thermistor are soldered to the slip rings. (See Fig. 8 and Fig. 9a.)

All probes were calibrated and a typical calibration curve is shown in Fig. 23. Probe 1 was the first probe to be used. It was subsequently found that the calibration is strongly dependent on the flow temperature. Furthermore, the A.C. component of the thermistor output affects the accuracy of reading the D.C. component, particularly in turbulent flow regimes. Since temperature variations were observed when the system was operating in a recirculating mode, (see Chapter II.C), it was decided to use less sensitive probes.

Probe 2 and 3 meet this requirement. They have a very low frequency response due to their size and therefore the fluctuation of the D.C. output is decreased. In addition, a higher resistance (about 12 times larger) replaces the one originally used in the anemometry circuit (with Probe 1).

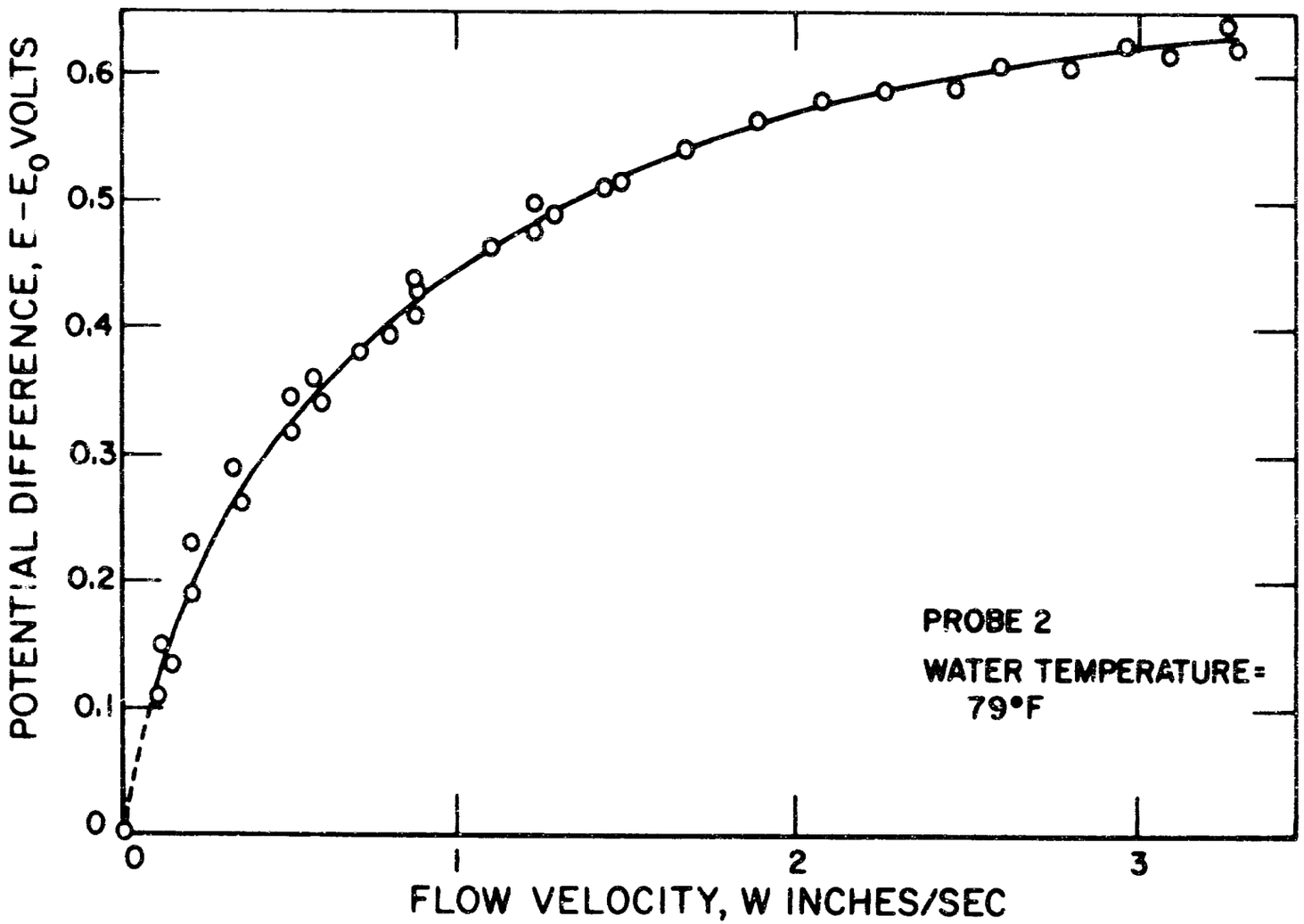

FIG. 23. TYPICAL CALIBRATION CURVE FOR A THERMISTOR PROBE.

Since the resistance is connected in series with the probe, the small differences in the flow temperature, and hence the probe resistance, are suppressed. In addition, a D.C. supply unit (0.01% ripple) is used to replace the two car batteries. The D.C. supply unit is operated at approximately 500 volts to maintain the potential difference applied to the thermistor probe unchanged with the higher series resistance (48K ohm).

The size of the resistance used to replace the original was carefully investigated so as not to affect the velocity measurements. Probe 2 and Probe 3 were then calibrated using the new resistance. Flow field measurements are successfully performed after these modifications are introduced and the results are presented in Chapter III.A.

For the final stability measurements, Probe 4 was used since the consideration is to obtain maximum frequency response and the D.C. components is of secondary effect. Hence, the smallest commercially available insulated probe was acquired and the series resistance (R) is chosen to give maximum frequency response. The resistance is selected so that the thermistor temperature at zero velocity is below the boiling point of the fluid.

The frequency response of all the probes is estimated by using an octave band analyzer to monitor their output in turbulent flow conditions. No attempt is made to measure the frequency

response by any other means, since it is believed that the results are satisfactory for indicating transition from laminar to turbulent regimes, which is the main purpose of this investigation.

The cut-off frequency for Probe 1 is found to be approximately five c.p.s., while for Probe 4 it is approximately ten c.p.s. The frequency response of the two other probes is almost an order of magnitude lower than that of Probe 1 and Probe 4. These results agree favorably with the preliminary calculations based on the probe properties.

APPENDIX C

HYDROGEN BUBBLES

A technique of flow visualization in water was introduced in the early part of the last decade. This technique is performed by using a fine wire as one end of a D.C. circuit to electrolize water. The technique is usually called "the hydrogen bubble visualization technique," since a negative voltage is usually used in the flow field to introduce hydrogen bubbles. (Oxygen bubbles from the positive electrode may also be used, but the hydrogen is usually preferred, since the volume of the hydrogen generated is twice as much for a given current.) The other end of the D.C. circuit is located somewhere else in the water tunnel.

In using the hydrogen bubble technique, one has a great number of possibilities which, if employed correctly, can result in obtaining three dimensional as well as transient information about the flow. In addition, quantitative information can be obtained if the fluid flow visualization is recorded on still photographs or movies. Recently the hydrogen bubble technique was also extended to be used in other working fluids such as glycerin-water mixtures.

A straight wire in the flow field will produce a sheet of bubbles. If the same wire is supplied with a pulsed current the

determination of one-dimensional velocity fields becomes possible. A wire that is insulated at intervals of its span will produce streak lines which can be used for flow visualization. A more convenient way of doing the same thing is by using a kinked wire. By using such a wire and orienting the kinks in the direction of the flow, the bubbles will be swept only at the peaks of the kinks. The use of kinked (or intervally insulated wires) with pulsed current will produce what is called combined-time-streak markers. Such markers can be used to determine the stream lines as well as the velocity field.

1. Apparatus

A D.C. power supply, capable of supplying up to 500 volts and up to 0.100 amp, is used. Two probes were constructed from 1/4-inch stainless steel tubing. The probes are shaped in the form of an "h" with a wire span of six inches. The probes were then completely insulated with electrical insulating tape. A 0.0015 inch platinum-10% rhodium annealed wire was then silver soldered to the prongs of the probe. The prongs were then insulated with RTV. A 0.004 inch wire made of the same material was kinked using a gear and rack of small size (approximately 1/16 inch pitch) and was then mounted on the other probe in a manner similar to the first one.

Three 500 watt flood lamps were used for lighting. A dark background was introduced for better visibility of the bubbles.

To pulse the supply current the microswitch and gear pulley used to measure the rotational speed of the pipe are used.

Since it was observed that the wires tend to produce large size bubbles after a period of operation has elapsed, different methods were used to remove the large bubbles from the wire. The method that was found to be most effective is reversing the polarity of the wire. Based on this, it was decided to use the other probe in place of the positive electrode and hence to be able to clean the probes by using them alternately.

The probe used is then placed in such a way as to have the wire stretched across the horizontal diameter of the rotating pipe at its exit plane in the open tank. Movies and still photographs are used to record and study the flow field.

2. Experimental Results

The straight wire was used with a pulsed current to visually determine the velocity profile. Photographs such as the one shown in Fig. 24, taken while using this technique, are then studied quantitatively. It was observed that the axial mean velocity profile is independent of rotation up to a swirl ratio of approximately four. The results obtained agree favorably with the ones measured with the hot-thermistor anemometry.

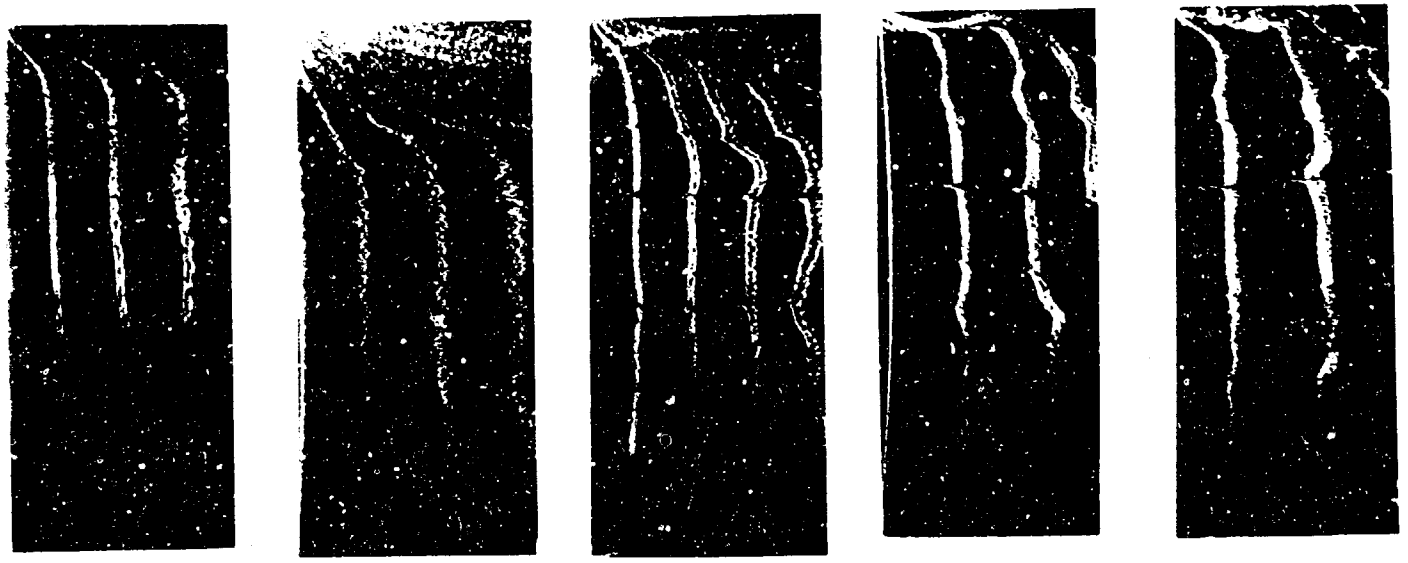

FIG. 24. MEAN AXIAL VELOCITY PROFILES FOR INCREASING AXIAL REYNOLDS NUMBERS WITH NO ROTATION ($N_{R\theta} = 0$), OBTAINED BY USING HYDROGEN BUBBLES.

Hydrogen bubbles were also used to determine the transition from laminar to turbulent flow regimes. The kinked wire was used in this group of experiments to produce streak lines in the flow field. Figure 25 shows a series of photographs taken in the course of these experiments. The agreement of these results with the hot-thermistor anemometry and dye streaks visualization is found to be very satisfactory.

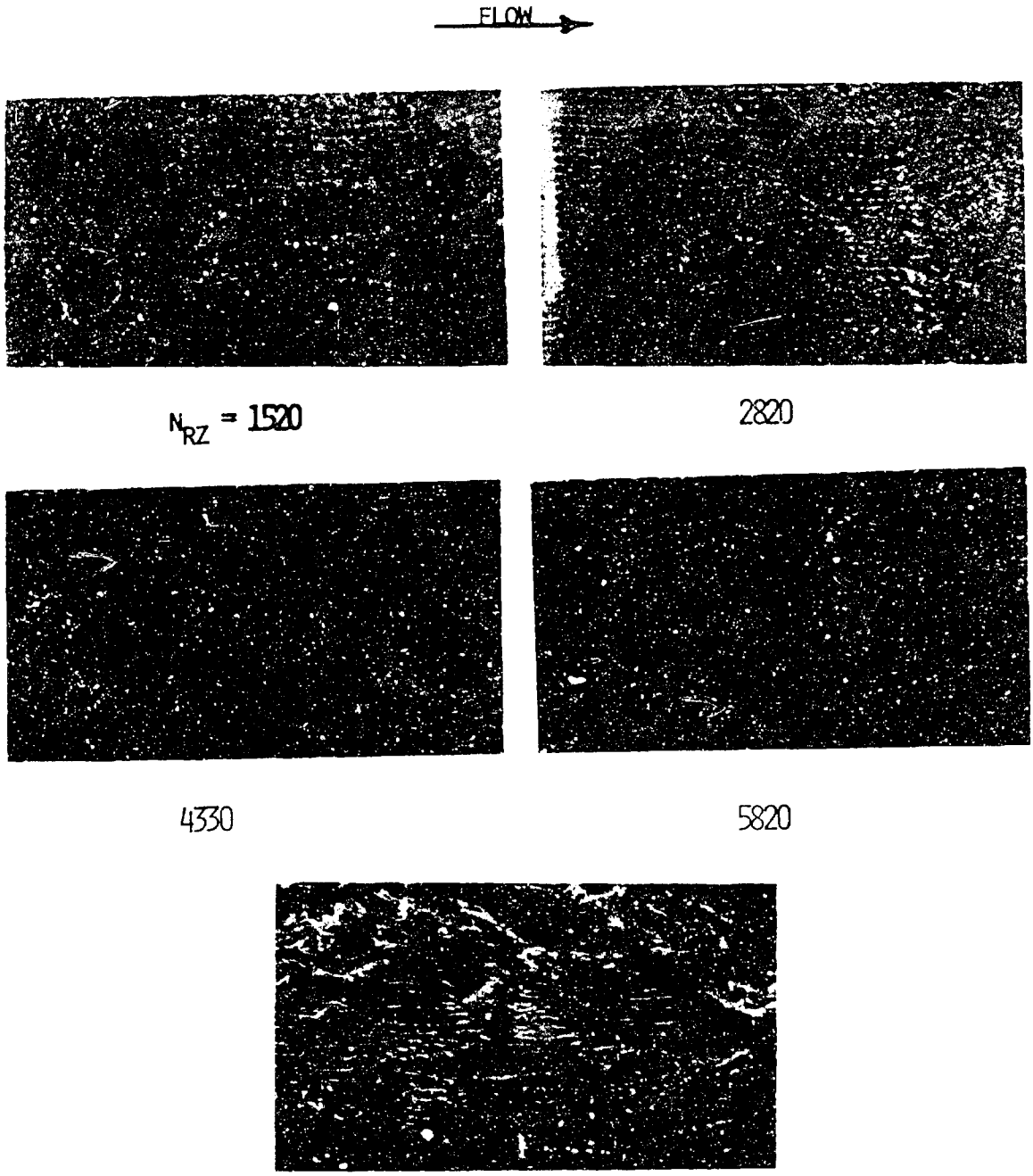

FIG. 25. HYDROGEN BUBBLE STREAKS FOR INCREASING AXIAL REYNOLDS NUMBERS WITH NO ROTATION ($N_{R\theta} = 0$)

REFERENCES

1. Reynolds, O., 1883, "An Experimental Investigation of the Circumstances which Determine whether the Motion of Water Shall be Direct or Sinuous, and of the Law of Resistance in Parallel Channels," Phil. Trans. Roy. Soc. 174, 935. (Also Sci. Papers, 2, 51.)

2. Sexl, Th., 1927, "Zur Stabilitätsfrage der Poiseuilleschen und Cuetteschen Strömung," Ann. Phys. 83, 835.

3. Sexl, Th., 1927, "Über dreidimensionale Störungen der Poiseulleschen Strömung," Ann. Phys. 84, 807.

4. Pekeris, C. L., 1948, "Stability of the Laminar Flow through a Straight Pipe of Circular Cross-Section to Infinitesimal Disturbances which are Symmetrical about the Axis of the Pipe," Proc. Nat. Acad. Sci., U.S., 34, 285.

5. Sexl, Th. and Spielberg, K., 1958, "Zum Stabilitätsproblem der Poiseuille - Strömung," Acta. Phys. Austriaca, 12, 9.

6. Corcos, G. M. and Sellars, J. R., 1959, "On the Stability of Fully Developed Flow in a Pipe," J. Fluid Mech. 5, 97.

7. Lessen, M., Gandler, S., and Liu, T., 1968, "Stability of Pipe Poiseuille Flow," Phys. Fluids 11, 1404.

8. Gill, A. E., 1965, "On the Behavior of Small Disturbances to Poiseuille Flow in a Circular Pipe," J.Fluid Mech. 21, 145.

9. Leite, R. J., 1959, "An Experimental Investigation of the Stability of Poiseuille Flow," J. Fluid Mech. 5, 81.

10. Fox, J. A., Lessen, M. and Bhat, W. V., 1968, "Experimental Investigation of the Stability of Hagen-Poiseuille Flow," Phys. Fluids 11, 1.

11. Rotta, J., 1956, "Experimenteller Beitrag zur Enstenung turbulenter Strömung im Rohr," Ing. Archiv. 24, 4, 258.

12. Orr, W. McF., 1907, "The Stability or Instability of Steady Motions of Liquid, Part II: A Viscous Liquid," Proc. Roy. Irish Acad. A., 27, 69.

References (Cont'd)

13. Joseph, D. D., and Carmi, S., 1969, "Stability of Poiseuille Flow in Pipes, Annuli, and Channels," Quarterly of Applied Mathematics, 16, 575.

14. Rayleigh, Lord, 1916, "On the Dynamics of Revolving Fluids," Proc. Roy. Soc. A, 93, 148 (also Sci. Papers 6, 447).

15. Taylor, G. I., 1923, "Stability of a Viscous Liquid Contained between Two Rotating Cylinders," Phil. Trans. Roy. Soc. A, 223, 289.

16. Sparrow, E. M., Munro, W. D., and Jonsson, V. K., 1964, "Instability of the Flow between Rotating Cylinders: the Wide-Gap Problem," J. Fluid Mech., 20, 35.

17. Coles, D., 1965, "Transition in Circular Couette Flow," J. Fluid Mech., 21, 385.

18. Shultz-Grunow, F., 1959, "On Stability of Couette Flow," ZaMM, 39, 101.

19. Chandrasekhar, S., 1961, Hydrodynamic and Hydromagnetic Stability, Oxford University Press.

20. Di Prima, R. C., 1960, "The Stability of a Viscous Fluid between Rotating Cylinders with an Axial Flow," J. Fluid Mech. 9, 621.

21. Chandrasekhar, S., 1960, "The Hydrodynamic Stability of Inviscid Flow between Coaxial Cylinders," Proc. Nat. Acad. Sci., Wash., 46, 137.

22. Krueger, E. R., and Di Prima, R. C., 1964, "The Stability of Viscous Fluid between Rotating Cylinders with an Axial Flow," J. Fluid Mech., 19, 528.

23. Datta, S. K., 1965, "Stability of Spiral Flow between Concentric Circular Cylinders at Low Axial Reynolds Number," J. Fluid Mech., 21, 635.

24. Howard, L. N., and Gupta, A. S., 1962, "On the Hydrodynamic and Hydromagnetic Stability of Swirling Flows," J. Fluid Mech., 14, 463.

References (Cont'd)

25. Hughes, T. H., and Reid, W. H., 1968, "The Stability of Spiral Flow between Rotating Cylinders," Phil. Trans. Roy. Soc. A., 263, 57.

26. Ludwieg, H., 1960, "Stabilität der Strömung in einem zylindrischen Ringraum," Z. Flugwiss 8, 135.

27. Ludwieg, H., 1961, "Ergänzung zu der Arbeit:'Stabilität der Strömung in einem zylindrischen Ringraum'," Z. Flugwiss 9, 359.

28. Ludwieg, H., 1962, "Zur Erklärung der Instabilität der über angestellten Deltaflügeln auftretenden Freien Wirbelkerne," Z. Flugwiss 10, 242.

29. Kiessling, I., 1963, "Über das Taylorsche Stabilitätsproblem bei zusätzlicher axialer Durchströmung der Zylindern," Deutsche Versuchsantalt für Luft-und Raumfahrt, Bericht 290.

30. Ludwieg, H., 1964, "Experimentelle Nachprüfung der Stabilitätstheorien für reibungsfreie Strömungen mit Schraubenlinienförmigen Stromlinien," Z. Flugwiss 12, 304.

31. Pedley, T. J., 1968,"On the Instability of Rapidly Rotating Shear Flows to Non-Axisymmetric Disturbances," J. Fluid Mech. 31, 603.

32. Pedley, T. J., 1969, "On the Instability of Viscous Flow in a Rapidly Rotating Pipe," J. Fluid Mech. 35, 97.

33. Strohl, J., 1969, "Hydrodynamic Stability of Poiseuille Flow in a Rotating Pipe," M.S. Thesis, Department of Mechanical and Aerospace Engineering, Illinois Institute of Technology.

34. White, A., 1964, "Flow of a Fluid in an Axially Rotating Pipe," J. Mech. Engineering Sci., 6, 47.

35. Cannon, J. N., and Kays, W. M., "Heat Transfer to a Fluid Flowing Inside a Pipe Rotating about Its Longitudinal Axis," Journal of Heat Transfer, Trans. ASME Series C, 91, 135.

36. Fejer, A. A., Lavan, Z., and Wolf, L., Jr., 1968, "Study of Swirling Fluid Flows," ARL Report No. 68-0173.

37. Lavan, Z., Nielsen, H., and Fejer, A. A., 1969, "Separation and Flow Reversal in Swirling Flows in Circular Ducts," Phys. Fluids, (to appear).

38. Lavan, Z., and Fejer, A. A., 1966, "Investigation of Swirling Flows in Ducts," ARL Report No. 66-0083.

39. Talbot, L., 1954, "Laminar Swirling Pipe Flow," J. Appl. Mech. 21, 1.

40. Hinze, J. O., 1959, Turbulence, McGraw-Hill Book Co., Inc.

41. Schlichting, H., 1968, Boundary-Layer Theory, McGraw-Hill Book Co., Inc.

42. Prandtl, L., and Tietiens, O. G., 1957, Applied Hydro- and Aero-Mechanics, Dover Publications.

43. Goldstein, S., 1965, Modern Developments in Fluid Dynamics, Vol. I and II, Dover Publications.

44. Lennemann, E., and Howard, J. H. G., 1969, "Unsteady Flow Phenomena in Rotating Centrifugal Impeller Passages," ASME Report No. 69-GT-35.

45. Baker, D. J., 1966, "A Technique for the Precise Measurement of Small Fluid Velocities," J. Fluid Mech., 26, 573.

46. Streeter, V. L., 1961, Handbook of Fluid Mechanics, McGraw-Hill Book Co., Inc.

47. Arthur, R. F., 1958, "Cooling of a Hemisphere by Mass Transfer," MIT Naval Supersonic Lab. Technical Report No. 310.

48. Bernicker, R. P., 1959, "An Investigation of Porous Wall Cooling," MIT Naval Supersonic Lab. Technical Report No. 393.

49. Hill, J. A. F., 1956, "The Permeability of Porous Walls," MIT Naval Supersonic Lab. A-R Memo No. 161, MTP Internal Tech. Memo No. 4.

50. Lumley, J. L., 1962, "The Constant Temperature Hot-Thermistor Anemometer," ASME Symposium on Measurement in Unsteady Flow, 75.

51. Lane, R. S., and Keller, R. B., 1967, "A Thermistor Probe for Low Velocity Flow Measurements," ASME Symposium on Fluidics, 251.

BIBLIOGRAPHY

1. Batchelor, G. K., and Gill, A. E., 1962, "Analysis of the Stability of Axisymmetric Jets," J. Fluid Mech. 14, 529.

2. Betchov, R., and Criminale, W. O., Jr., 1967, Stability of Parallel Flows, Academic Press.

3. Cannon, J. N., 1965, "Heat Transfer from a Fluid Flowing Inside a Rotating Cylinder," Ph.D. Thesis, Department of Mechanical Engineering, Stanford, University.

4. Chandrasekhar, S., 1954, "The Stability of Viscous Flow between Rotating Cylinders," Mathematika, 1, 5.

5. Davis, W., and Fox, R. W., 1967, "An Evaluation of the Hydrogen Bubble Technique for the Quantitative Determination of Fluid Velocities within Clear Tubes," Journal of Basic Engineering Trans. ASME Series D 89, 771.

6. kovasznay, L. S. G., 1954, "Physical Measurements in Gas Dynamics and Combustion," High Speed Aerodynamics and Jet Propulsion, Sec. F, Vol. 9, Princeton University Press.

7. Lamb, H., 1945, Hydrodynamics, Dover Publications.

8. Lessen, M., Fox, J. A., Bhat, W. V., and Liu, T. Y., 1964, "Stability of Hagen-Poiseuille Flow," Phys. Fluids 7, 1384.

9. Levin, V. B., 1964, "The Stabilizing Effect of Rotation on a Turbulent Flow," Teplofizika Vysokikh Temperatur, Vol. 2, No. 6, 804.

10. Ludwieg, H., 1965, "Erklärung des Wirbelaufplatzens mit Hilfe der Stabilitätsteorie für Strömugen mit Schraubenlinienförmigen Stromlinien," Z. Flugwiss 13, 437.

11. Rayleigh, Lord, 1880, "On the Stability, or Instability, of Certain Fluid Motions," Proc. Lond. Math. Soc. 11, 57, (also Sci. Papers 1, 474).

12. Rayleigh, Lord, 1892, "On the Question of the Stability of the Flow of Fluids," Phil. Mag. 34, 59 (also Sci. Papers 3, 575).

13. Reynolds, O., 1895, "On the Dynamical Theory of Incompressible Viscous Fluids and the Determination of the Criterion," Phil. Trans. Roy. Soc. A., 186, 123.

14. Schraub, F. A., Kline, S. J., Henry, J., Runstadler, P. W., and Littell, A., Jr., 1965, "Use of Hydrogen Bubbles for Quantitative Determination of Time Dependent Velocity Fields in Low-Speed Water Flows," Journal of Basic Engineering, Trans. ASME Series D, 87, 429.

15. Traugott, S. C., 1958, "Influence on Solid-Body Rotation of Screen-Produced Turbulence," NACA Tech. Note No. 4135.

UNCLASSIFIED
Security Classification

DOCUMENT CONTROL DATA - R & D

(Security classification of title, body of abstract and indexing annotation must be entered when the overall report is classified)

1. ORIGINATING ACTIVITY *(Corporate author)*
Illinois Institute of Technology
10 West 35th Street
Chicago, Illinois 60616

2a. REPORT SECURITY CLASSIFICATION
UNCLASSIFIED

2b. GROUP

3. REPORT TITLE

On the Stability of Flow in Rotating Pipes

4. DESCRIPTIVE NOTES *(Type of report and inclusive dates)*
Scientific. Final.

5. AUTHOR(S) *(First name, middle initial, last name)*

Hassan M. Nagib; Ludwig Wolf, Jr.; Dr. Zalman Lavan; Dr. Andrew A. Fejer

6. REPORT DATE	7a. TOTAL NO. OF PAGES	7b. NO. OF REFS
October 1969	106	66

8a. CONTRACT OR GRANT NO.	9a. ORIGINATOR'S REPORT NUMBER(S)
F33 615-67-C-1406	
b. PROJECT NO. 7116	
c. DoD element 61102F	9b. OTHER REPORT NO(S) *(Any other numbers that may be assigned this report)*
d. DoD Subelement 681308	ARL 69-0176

10. DISTRIBUTION STATEMENT

1. This document has been approved for public release and sale; its distribution is unlimited.

11. SUPPLEMENTARY NOTES	12. SPONSORING MILITARY ACTIVITY
TECH OTHER	Aerospace Research Laboratories (ARE) Wright-Patterson AFB, Ohio 45433

13. ABSTRACT

The stability of flow in rotating pipes is investigated experimentally. The results of this investigation also have a bearing on the stability of flow in the core of swirling flows in stationary ducts and free vortices. Solid body rotation is found to have a destabilizing effect when superposed on a pipe entrance region axial velocity profile. The range of swirt ratios up to four is investiagted using two different approaches: dye streaks visualization and hot-thermistor anemometry. As the swirl ratio is increased from zero to four, the axial Reynolds number at which laminar flow breaks down decreases from 2500 to 900. These results agree in trend with the limit axial Reynolds number value of 82.9 that was recently obtained by analytical investigations of the stability of a viscous fully developed axial velocity profile subject to a rapid, almost rigid rotation in pipes. The present results also suggest that the destablizing trend due to solid body rotation may also hold for other axial velocity profiles and indicates a possible new mechanism of confined flow instability that takes place at lower Reynolds numbers than previously believed possible.

DD FORM 1 NOV 68 1473

UNCLASSIFIED
Security Classification

14. KEY WORDS	LINK A		LINK B		LINK C	
	ROLE	WT	ROLE	W	ROLE	WT
Flow Stability Rotating Flow Swirl Flows Hot-Thermistor Anemometry Solid Vortex Transition Reynolds Number Flow visualization						